

Long-Term Monitoring of Hydrological Dynamics and Phytoplankton Biomass Indicator in Three Shellfish Ecosystems of the English Channel (2000-2024)

Julia Sosinski^{1*}, Stéphanie Petinay¹, Jean-Louis Blin¹

¹ Synergie Mer & Littoral, Centre Expérimental, Zone conchylicole, 33 rue du Banc du Nord, Blainville-Sur-Mer 50560, France

Correspondence to: Julia Sosinski (jsosinski@smel.fr)

Abstract. This data paper presents a harmonized and quality-controlled dataset resulting from 24 years (2000–2024) of monthly monitoring at three coastal stations in Normandy, France: Blainville-sur-Mer, Saint-Vaast-la-Hougue, and Utah Beach. The dataset includes measurements of key physico-chemical parameters (temperature, salinity, pH, dissolved oxygen), biogeochemical variables (dissolved nutrients: nitrate, ammonium, phosphate, and silicate), and biological indicators (chlorophyll *a* concentration, phytoplankton fluorescence). Sampling was conducted using consistent protocols across stations, allowing for long-term comparison. All data have undergone validation and standardization to ensure their usability for environmental assessment and modeling purposes. The dataset provides valuable insights into the evolution of coastal water quality under the influence of climate change and anthropogenic pressures. Notable trends include increasing winter temperatures (especially since 2010), progressive ocean acidification at Blainville-sur-Mer, and changing nutrient regimes across the region, with a marked phosphate decline and spatial contrasts in nutrient limitation (phosphorus-limited on the East coast, nitrogen-limited on the West coast). These long-term observations are critical for understanding ecosystem dynamics, supporting coastal management strategies, and informing sustainable aquaculture development. The dataset is openly available and intended to support further interdisciplinary research in marine science and environmental policy.

1. Introduction

Located at the interface between land and ocean, coastal ecosystems are highly productive areas essential for the survival of many marine species (Barbier *et al.*, 2011). However, these environments are under increasing pressure from human activities, such as eutrophication, pollution, and changes to coastal and marine landscapes. These threats affect both benthic and pelagic habitats, thereby disrupting ecological balances (Sala *et al.*, 2000 ; Dudgeon *et al.*, 2006 ; Halpern *et al.*, 2007 ; Barbier *et al.*, 2011 ; Ovaskainen *et al.*, 2019).

Since the 1950s, the widespread use of fertilizers in intensive agricultural practices has led to an increase in nutrient inputs into European coastal waters (Vermaat *et al.*, 2008). Over the decades, numerous programs have been implemented to limit these discharges, but while the effects on phosphorus inputs have been notable (Claussen *et al.*, 2009), nitrogen inputs remain very high (Garnier *et al.*, 2019). These inputs influence not only the concentration of nutrients but also their stoichiometry (Martin *et al.*, 2008 ; Watanabe *et al.*, 2017 ; Meybeck *et al.*, 2018). These imbalances lead to changes in the productivity of phytoplankton communities, which are at the base of the food web, as well as in their composition (Shen, 2001 ; Cadée & Hegeman, 2002 ; Smith, 2006 ; Lefebvre *et al.*, 2011 ; Leruste *et al.*, 2019).

Nutrient inputs, alongside other environmental factors such as light availability, temperature, water residence time, and river discharge, play a critical role in driving phytoplankton blooms (Heisler *et al.*, 2008). These blooms are vital for shellfish ecosystems, serving as an essential food source for farmed bivalves (Sonier *et al.*, 2016 ; Filgueira *et al.*, 2016). However, studies have reported a slowdown in primary production, including phytoplankton blooms, due to changing environmental conditions (Romero *et al.*, 2016).

Climate change significantly influences coastal systems through various physical and chemical processes (Kirby *et al.*, 2009). Beyond the well-documented direct effects of rising temperatures on marine organisms (Beaugrand, 2004), warming also affects water stratification, which alters the vertical exchange of nutrients and dissolved oxygen (Sarmiento & Gruber, 2006). This can lead to an increased occurrence of hypoxic or anoxic events in coastal waters (Diaz, 2001 ; Selman *et al.*, 2008). Furthermore, atmospheric circulation—through changes in sea level pressure, wind direction, and intensity—impacts oceanic currents, which play a key role in the horizontal transport of nutrients and dissolved oxygen in these ecosystems (Cloern, 2001 ; Reid *et al.*, 2003).

Since the early 2000s, the HYDRONOR observatory has been dedicated to monitoring the water quality of shellfish farming areas in the Cotentin Peninsula (Normandy). This observatory provides one of the longest and most comprehensive time series on hydrobiological parameters available for this region. The objective of the present study is to offer a robust dataset of key environmental variables at three representative shellfish stations—Blainville-sur-Mer, Saint-Vaast-La-Hougue, and Utah Beach—monitored by HYDRONOR. Over 20 years of high-frequency data have been compiled, offering robust insights into coastal dynamics in response to anthropogenic pressures and climate variability.

This dataset is particularly valuable due to its regional scale, high temporal resolution, and methodological consistency. It complements national initiatives such as the SOMLIT program (Service d’Observation en Milieu Littoral), which monitors long-term trends in coastal waters at key research sites across France. While SOMLIT stations such as Luc-sur-Mer (Baie de Seine) and Roscoff provide critical data on large-scale trends, HYDRONOR offers a higher spatial resolution within a single department with a focus on shellfish-farming ecosystems. As such, it bridges the gap between broader-scale observations and local aquaculture management needs.

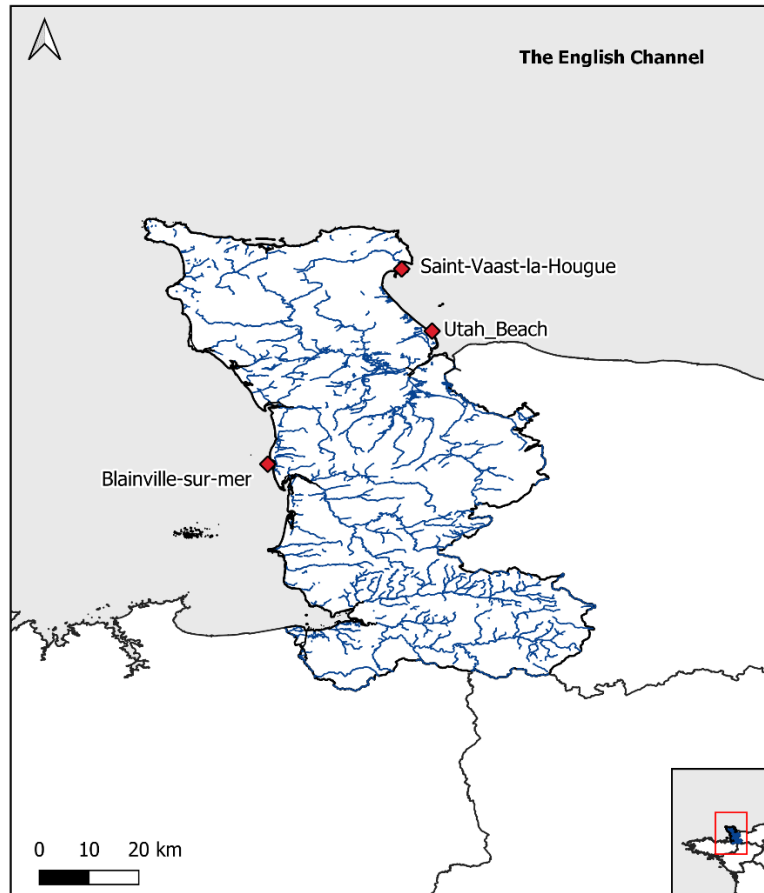
2. Material and methods

2.1. Sampling sites and strategies

Among the coastal stations monitored by the HYDRONOR observatory, three were selected for this dataset: Blainville-sur-Mer, Saint-Vaast-la-Hougue, and Utah Beach. These stations were chosen primarily because they offer the most complete and continuous datasets since the beginning of the monitoring program in 2000, ensuring the robustness and reliability of long-term analyses. In addition to their data quality, these sites represent contrasting environmental conditions that allow for the exploration of a representative gradient along the Normandy coastline. Two of these areas are located in open ecosystems, heavily exploited by oyster farming activities: Saint-Vaast-la-Hougue, in the eastern part of the department, and Blainville-sur-Mer, in the western part. The third area, Utah Beach, is located in the enclosed environment of the Baie des Veys, under strong anthropogenic influence (Figure 1). These include intensive agricultural activity in the watershed (particularly livestock farming and maize cultivation), leading to diffuse nutrient inputs via river discharges (notably from the Douve, Taute, and Vire rivers) (Grangere, 2004 ; Chenel, 2025).

75

The analysis focused on key environmental variables directly involved in the stoichiometry of primary production: dissolved inorganic nitrogen ($\text{DIN} = \text{NO}_3^- + \text{NO}_2^- + \text{NH}_4^+$), orthophosphate (PO_4^{3-}), and reactive silicate (Si(OH)_4), as well as chlorophyll *a*, used as a proxy for phytoplankton biomass. These variables were selected due to their ecological relevance and the consistency of their measurement across the full study period and all three stations.



80

Figure 1: Location of the sampling stations along the French coast in the English Channel (Blainville-sur-mer, Saint-Vaast-La-Hougue, Utah Beach). The blue lines represent the river network of the department.

2.2. Sample analysis

The samples were collected at a depth of 1 meter using a 5L Niskin bottle, twice a month, one hour before or after high tide. Chlorophyll *a* concentrations were determined following filtration of three 100 mL aliquots through glass fiber filters (Whatman GF/F, nominal pore size 0.7 μm). Filters were stored frozen (-20°C) and extracted in 90% acetone for 12–24 h in the dark at 4°C . Measurements were performed using a Turner Designs fluorometer, following the method described by [Strickland & Parsons \(1972\)](#). Results are expressed in $\mu\text{g L}^{-1}$. Nutrients were measured via spectrophotometry. Mineral nitrogen was quantified through ammonium (NH_4^+), nitrite (NO_2^-), and nitrate (NO_3^-). Only the assimilable form of phosphorus, orthophosphate (PO_4^{3-}), was quantified, as well as silicates (Si(OH)_4). The methods are detailed in [Table 1](#).

90

Nutrient samples were pre-filtered at the time of collection using a $50\ \mu\text{m}$ mesh filter mounted directly on the Niskin bottle to remove large particulate matter. After collection, all samples were centrifuged for 10 minutes at 4200 rpm to eliminate residual suspended particles. This approach ensures that only the dissolved

95 fraction is analyzed. Samples were then stored at 4 °C in the dark and analyzed within 4 hours after sampling to minimize any transformation or degradation of the compounds.

Table 1: Analytical Methods for the Determination of Nutrients in seawater samples

Molecule	References	Principe
Ammonium (NH ₄ ⁺)	Standard NF T 90-015-2 (January 2000): Water testing – Determination of ammoniacal nitrogen	In an alkaline medium (10.4 < pH < 11.5), the ammonium ion reacts with phenol and hypochlorite to form monochloramine. This compound, in the presence of nitroprusside as a catalyst, leads to the formation of indophenol blue. The absorption is measured using a spectrophotometer at 630 nm.
Nitrate (NO ₃ ⁻) / Nitrite (NO ₂ ⁻)	<u>Aminot & Chaussepied, 1983</u> <u>Bendschneider & Robinson, 1952</u> <u>Aminot & Kerouel, 2004</u>	The selected method is based on the determination of NO ₂ ⁻ ions obtained through the quantitative reduction of NO ₃ ⁻ ions. In practice, the measurement reflects the sum of the concentrations of both ions, from which the nitrite concentration is deducted separately, without reduction. The reduction is carried out by passing the sample through a cadmium column treated with copper. After nitrate reduction (Griess reaction), measurement is performed based on the determination of nitrite ions. Nitrite ions form a diazo compound with sulfanilamide in an acidic medium (pH < 2), which then reacts with N-naphthyl-ethylenediamine to form a pink dye absorbing at 543 nm.
Orthophosphate (PO ₄ ³⁻)	<u>Aminot & Chaussepied, 1983</u> <u>Murphy & Riley, 1962</u>	Phosphate ions react with ammonium molybdate in the presence of antimony to form a complex that is then reduced by ascorbic acid; this reduced form, with a blue coloration, has a maximum absorption at 885 nm. This blue compound contains phosphorus, molybdenum, and antimony in atomic proportions of 1-12-1. Polyphosphates and organic phosphorus are not measured by this method.
Orthosilicic acid (Si(OH) ₄)	<u>Aminot & Chaussepied, 1983</u> <u>Mullin & Riley, 1955</u> <u>Strickland & Parsons, 1972</u> <u>Aminot & Kerouel, 2004</u>	The colorimetric determination is based on the formation of a silicomolybdic complex which, after reduction, produces an intense blue coloration. Orthosilicic acid tends to form polymers, of which only the mono- and dimeric forms react with molybdate ions under the conditions of this method, making the term "reactive silicon" more appropriate. Under reaction conditions, colloidal silicates are measured together with dissolved silicates using this method.

Calibration standards were prepared using low-nutrient seawater and validated at the SMEL laboratory (Syndicat Mixte pour l'Équipement du Littoral, France), in accordance with the French standard AFNOR XP T90-210 (May 2009), which defines the protocol for the initial performance evaluation of analytical methods in environmental laboratories.

In situ temperature and salinity were recorded using a YSI 6600 multi-parameter probe, calibrated prior to each field campaign according to the manufacturer's instructions. Salinity calibration was performed using certified NaCl standards (35 PSU). The accuracy of the salinity sensor was ± 0.1 PSU, and for temperature ± 0.15 °C. The probe was systematically verified against atmospheric pressure measurements to ensure the reliability of barometric compensation, particularly for sensors sensitive to pressure fluctuations (e.g. pH or oxygen, if applicable). The pH was measured in the laboratory using a Mettler Toledo F2 pH-meter equipped with a LE420 glass electrode. The instrument was calibrated daily using standard buffer solutions (pH 4.00, 7.00, and 10.00 at 20 °C). Measurements were performed at a controlled temperature of 20 °C, on the NBS scale, without CO₂ equilibration. Water samples were stored in the dark at 4 °C and analyzed within 4 hours after collection to limit any biological or chemical alterations. To assess the potential limitation of primary production by nutrient availability, the standard molar ratios for dissolved inorganic nitrogen (DIN = ammonium + nitrite + nitrate), phosphate, and silicate were calculated and compared. These ratios were based on the biogenic matter composition described by [Redfield *et al.* \(1963\)](#) and [Brzezinski \(1985\)](#), which is Si:N:P = 16:16:1.

Additionally, to evaluate the analytical sensitivity and ensure proper data interpretation, the limits of detection (LD) and limits of quantification (LQ) were determined for each parameter based on method validation procedures carried out in accordance with the AFNOR XP T90-210 standard. These values are summarized in [Table 2](#).

Table 2: Limit of detection (LD) and limit of quantification (LQ) for the different parameters.

Parameter	LD ($\mu\text{mol}\cdot\text{L}^{-1}$)	LQ ($\mu\text{mol}\cdot\text{L}^{-1}$)
Ammonium (NH_4^+)	0.074 $\mu\text{mol}\cdot\text{L}^{-1}$	0.222 $\mu\text{mol}\cdot\text{L}^{-1}$
Nitrite (NO_2^-)	0.12 $\mu\text{mol}\cdot\text{L}^{-1}$	0.036 $\mu\text{mol}\cdot\text{L}^{-1}$
Nitrate (NO_3^-)	0.025 $\mu\text{mol}\cdot\text{L}^{-1}$	0.076 $\mu\text{mol}\cdot\text{L}^{-1}$
Orthophosphate (PO_4^{3-})	0.021 $\mu\text{mol}\cdot\text{L}^{-1}$	0.063 $\mu\text{mol}\cdot\text{L}^{-1}$
Orthosilicic acid ($\text{Si}(\text{OH})_4$)	0.059 $\mu\text{mol}\cdot\text{L}^{-1}$	0.178 $\mu\text{mol}\cdot\text{L}^{-1}$
Chlorophyll a	0.292 $\mu\text{g}\cdot\text{L}^{-1}$	0.875 $\mu\text{g}\cdot\text{L}^{-1}$

2.3. Data analysis

The entire dataset was analyzed using the R statistical software ([R Core Team, 2022](#)), with the TTAinterfaceTrendAnalysis package developed by [Devreker & Lefebvre \(2014\)](#). This package is specifically designed for the analysis of long-term environmental time series. It applies non-parametric statistical methods such as the Seasonal Kendall test and Sen's slope estimator, which are robust to non-normal data distributions, missing values, and outliers—characteristics commonly encountered in environmental datasets. The package enables the detection and quantification of monotonic trends, as well as the evaluation of seasonal and interannual variability.

This makes it particularly suitable for identifying long-term changes in parameters such as temperature, pH, and nutrient concentrations in coastal ecosystems.

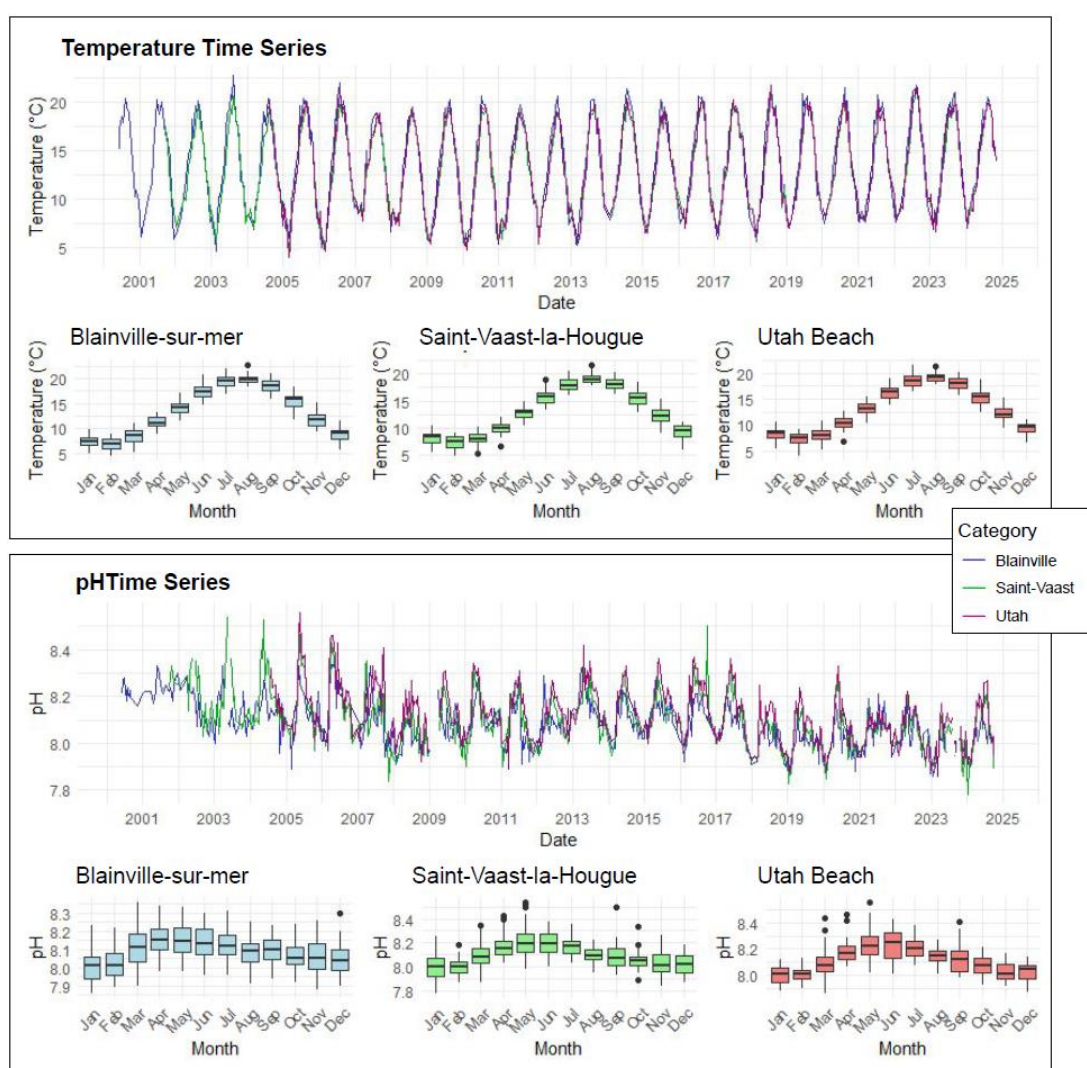
135

3. Results

3.1. Evolution of Physico-Chemical Parameters: Increase in winter temperature and pH

Figure 2 presents the monitoring of physico-chemical parameters. The monthly trends across the three stations show a similar pattern regarding temperature. However, the time series reveals a notable increase in winter temperatures. For instance, between 2009 and 2013, the average minimum temperatures at the three stations were around 5°C. In contrast, from 2013 to 2024, these minimum temperatures ranged between 6°C and 8°C across all stations.

140



145

Figure 2: Time Series and Monthly Averages of Temperature (°C) (top) and pH (bottom) from 2000 to 2024 at Blainville-sur-Mer, Saint-Vaast-la-Hougue, and Utah Beach. Boxplots show the 25th–75th percentile range (interquartile range, IQR), with the median as a horizontal line. Whiskers extend to $1.5 \times \text{IQR}$; points beyond are outliers.

Changes are also observed in seawater pH, which has gradually declined over the monitoring period (Figure 2). In the early 2000s, the lowest recorded pH remained above 8.0, whereas by 2024, it had decreased to

7.85. These trends over time are further illustrated by the anomaly plots presented in [Figure 3](#). The red anomalies for temperature represent values above the interannual averages (positive anomalies) and show an increasing frequency and intensity over time, particularly in recent years. For pH, the dominance of blue anomalies since 2017 indicates a progressive acidification, most noticeable at Blainville-sur-Mer, on the western coast, but also evident at the other two sites.

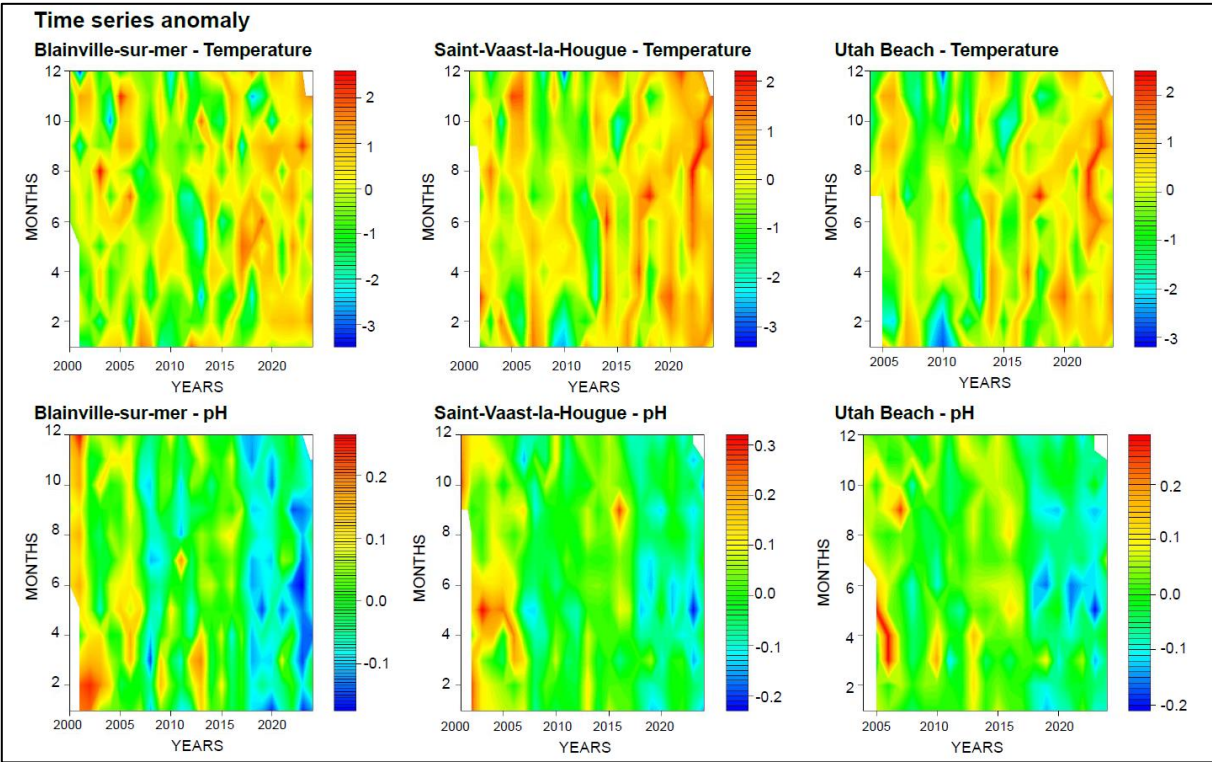
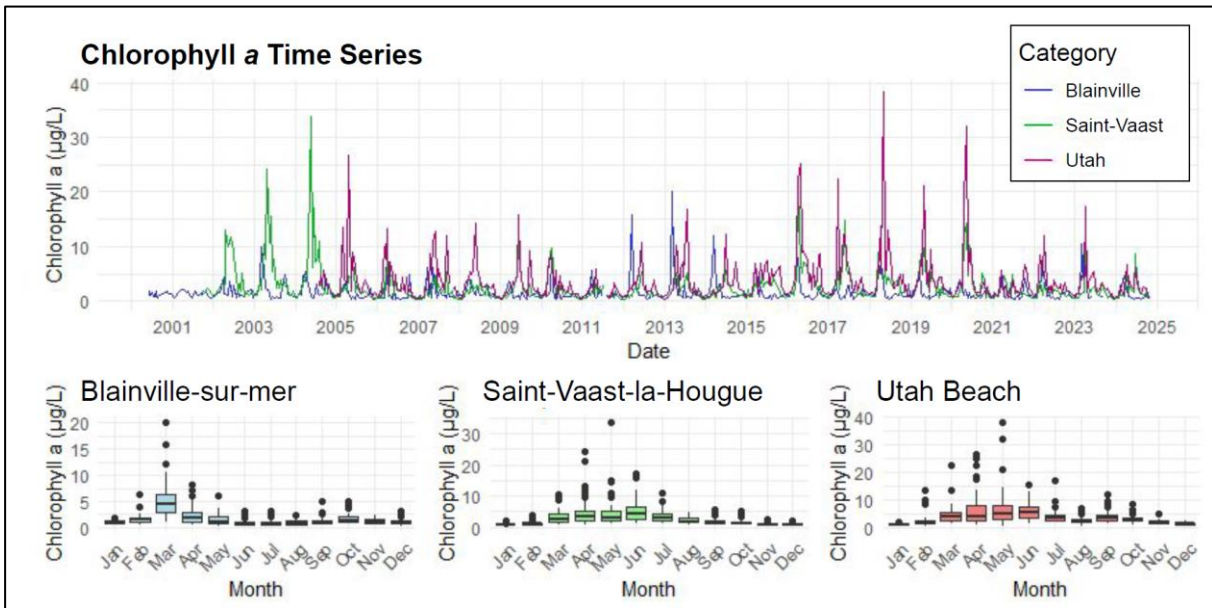


Figure 3: Monitoring of temperature (Top) and pH (Bottom) anomalies for the 3 stations. Anomalies are Calculated as Deviations from the Median (red : positive anomalies / blue : negative anomalies).

3.2. Spatial and Temporal Variability of Chlorophyll *a* Concentrations

Chlorophyll *a* concentrations are illustrated in [Figure 4](#). The stations located on the eastern coast, Saint-Vaast-la-Hougue and Utah Beach, exhibit the highest levels, with peaks exceeding 20 $\mu\text{g/L}$, compared to a



maximum of 10 $\mu\text{g/L}$ at Blainville-sur-Mer. On the western coast, the annual bloom is clearly visible, marked by an increase in chlorophyll *a* concentrations every March.

Figure 4: Time Series and Monthly Averages of chlorophyll *a* ($\mu\text{g.L}^{-1}$) from 2000 to 2024 at Blainville-sur-Mer, Saint-Vaast-la-Hougue (Tocquaise), and Utah Beach.

Since 2020, a drastic decrease in chlorophyll *a* concentrations has been observed on the eastern coast. This trend is confirmed by [Figure 5](#), which highlights values below the median for this period. Moreover, the predominance of green in the Blainville graph, compared to blue for the other two stations, underscores the differences between the western and eastern coastal ecosystems.

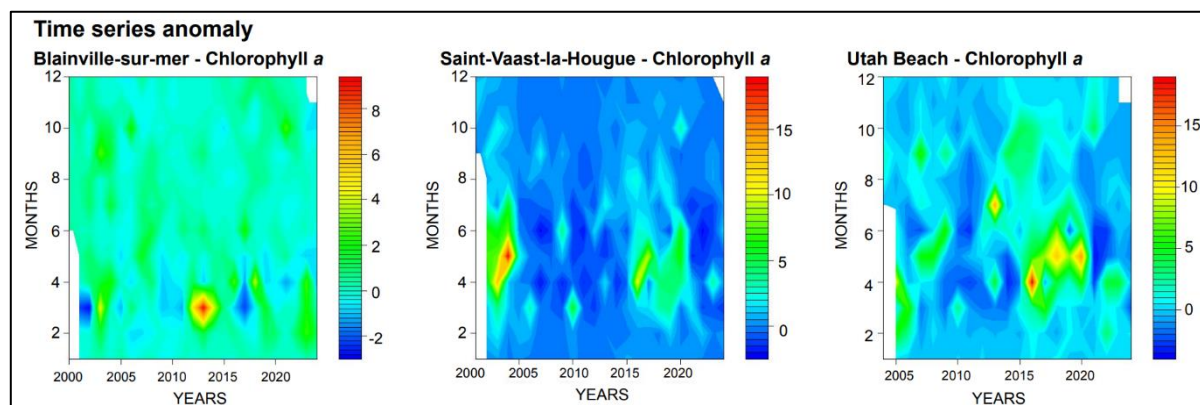


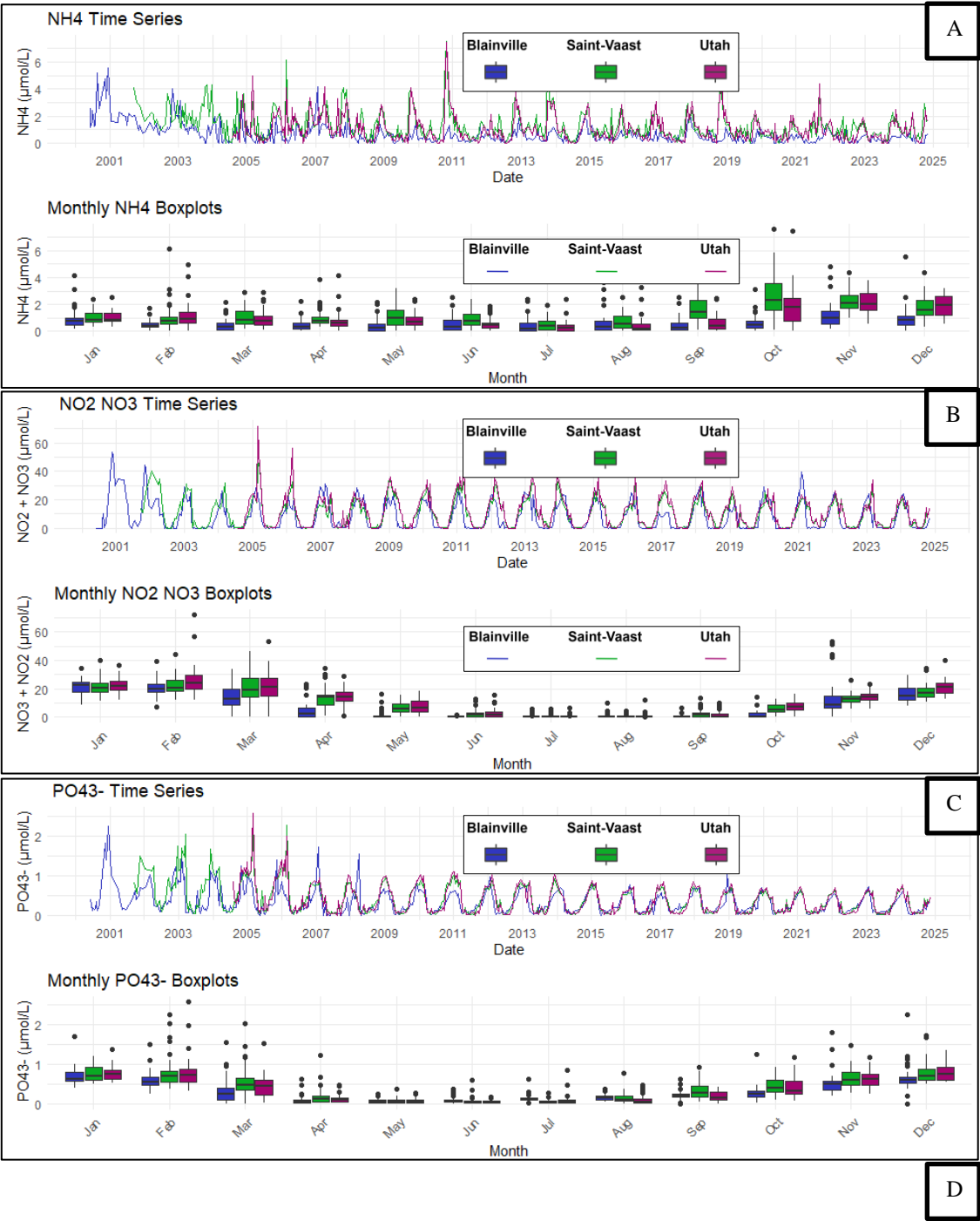
Figure 5: Monitoring of Chlorophyll *a* anomalies for the three Stations: Blainville-sur-Mer, Saint-Vaast-la -Hougue (Tocquaise), and Utah Beach. Anomalies are Calculated as Deviations from the Median (red : positive anomalies / dark blue : negative anomalies).

3.3. Spatial and temporal variability of inorganic nutrient concentration

The evolution and trends of dissolved nutrients are illustrated in [Figure 6](#). Ammonium shows the most marked variations between the stations, with higher concentrations observed on the East coast (Saint-Vaast-la-Hougue), where values can exceed 2 $\mu\text{mol.L}^{-1}$, compared to the West coast (Blainville-sur-Mer), where maximum concentrations are closer to 1 $\mu\text{mol.L}^{-1}$. Ammonium levels tend to increase between September and December at all sites. Nitrites and nitrates exhibit more cyclical and synchronized seasonal variations across the three stations. Their concentrations are lowest in summer, then increase significantly during the winter, peaking in January at values exceeding 20 $\mu\text{mol.L}^{-1}$, before gradually decreasing in the spring. On the West coast, although the maximum concentrations are similar to those of the East coast, they decrease more rapidly once the winter peak is reached. As for orthophosphates and silicates, the trends follow a similar pattern to those of nitrates plus nitrites: concentrations rise in the autumn, peak in the winter, and decrease in the spring. For phosphate, concentrations rarely exceed 1 $\mu\text{mol/L}$, while silicates reach nearly 30 $\mu\text{mol/L}$ in winter, especially on the East coast. However, no difference was observed between the two coasts for silicates. Finally, the time series for phosphate highlights a gradual decline in concentrations over the past 15 years on both coasts.

[Figure 7](#) shows the seasonal decomposition of chlorophyll-*a* concentrations. A well-defined seasonal cycle is visible at each station, with spring peaks and summer declines. The long-term trend component reveals a gradual decrease in chlorophyll-*a* until around 2010, followed by a transient increase until 2015, and then a continued decline. Over the full 2000–2024 period, total chlorophyll-*a* concentrations decreased by 0.2 $\mu\text{g.L}^{-1}$ at

190 Blainville-sur-Mer, $3.0 \mu\text{g.L}^{-1}$ at Saint-Vaast-la-Hougue. The remainder components show moderate interannual variability.



195

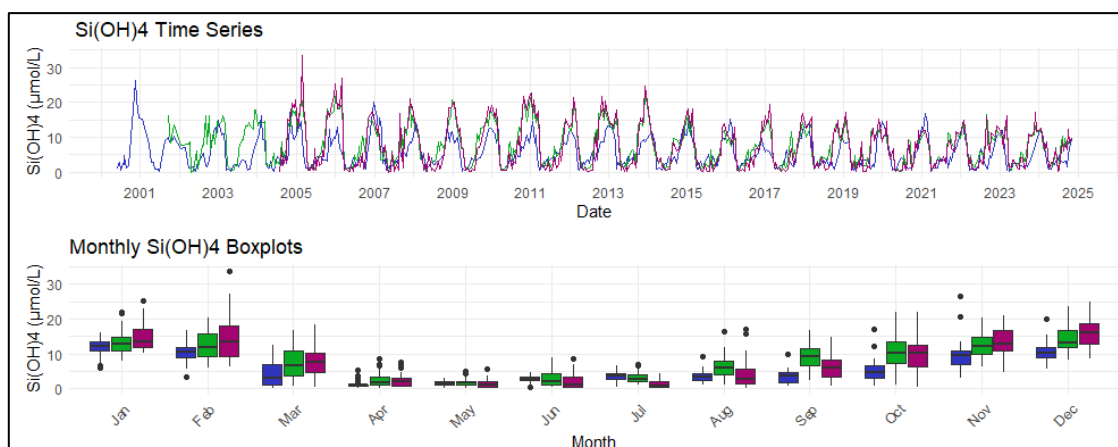


Figure 6: Time series and monthly averages of nutrient concentrations at the three stations (2000-2024): Blainville-sur-Mer, Saint-Vaast-la-Hougue, and Utah Beach. A: Ammonium (NH_4^+), B: Nitrites and Nitrates (NO_2^- , NO_3^-), C: Orthophosphate (PO_4^{3-}), D: Orthosilicic acid (Si(OH)_4).

200



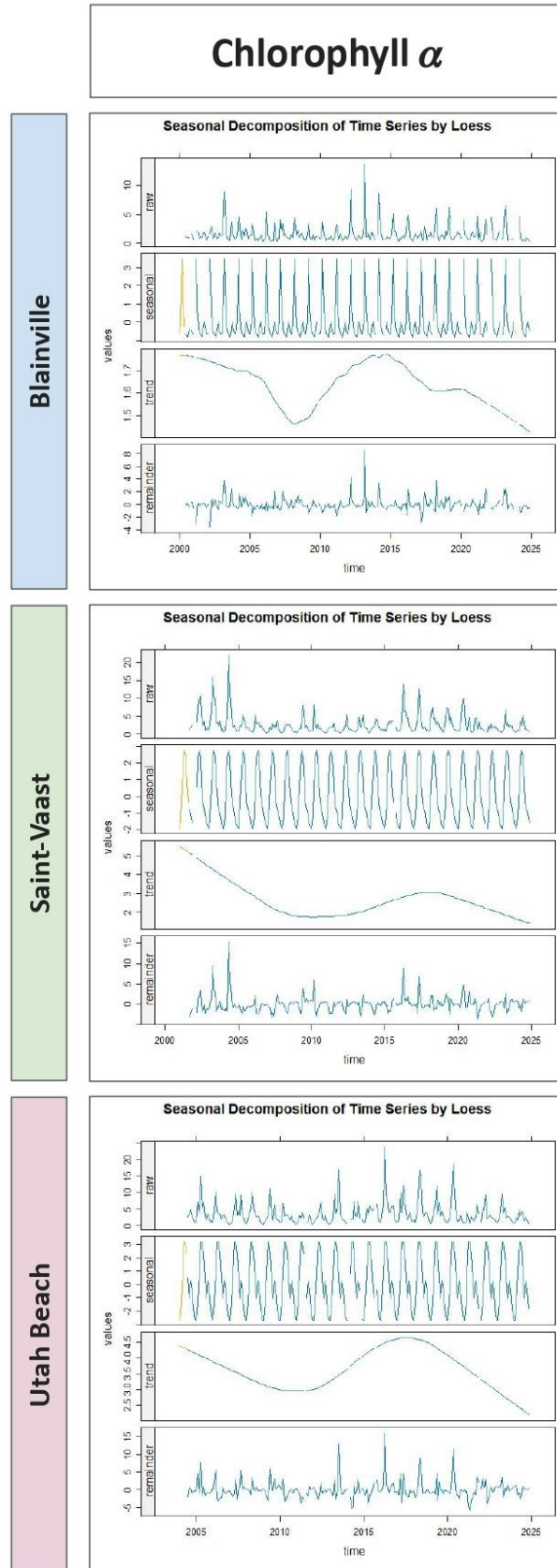


Figure 7: Seasonal Decomposition of Chlorophyll-a Concentrations ($\mu\text{g L}^{-1}$) from 2000 to 2024 at Blainville-sur-Mer, Saint-Vaast-la-Hougue, and Utah Beach. For each station, four panels are shown: the original time series (*Raw*), the seasonal component (*Seasonal*), the long-term trend (*Trend*), and the residuals (*Remainder*). The decomposition was performed using LOESS smoothing with the `TrendAnalysis` function from the `TTAinterfaceTrendAnalysis` R package

205

The seasonal decomposition of nitrogenous nutrients (ammonium, nitrite, and nitrate) are represented in the Figure 8. For nitrate and nitrite, a strong and consistent seasonal pattern is observed at all three stations, with pronounced winter maxima and summer minima. The seasonal signal remains stable over time, while the long-term trend indicates a general decline across all sites. Between 2000 and 2024, nitrate and nitrite concentrations decreased by approximately $6.0 \mu\text{mol.L}^{-1}$ at Blainville-sur-Mer and Saint-Vaast-la-Hougue, and by $4.0 \mu\text{mol.L}^{-1}$ at Utah Beach. Ammonium also shows a seasonal signal, although less regular and with more interannual variability. Its long-term trend indicates a decrease of about $1.5 \mu\text{mol.L}^{-1}$ at Blainville-sur-Mer, $1.0 \mu\text{mol.L}^{-1}$ at Saint-Vaast-la-Hougue, and $0.4 \mu\text{mol.L}^{-1}$ at Utah Beach. The remainder component for ammonium is more variable than for nitrate and nitrite, suggesting a greater influence of short-term events.

The seasonal decomposition of orthophosphates and silicates (Figure 9) reveals a clear and recurrent annual cycle at all stations, characterized by peak concentrations in winter and minimum levels in summer. This seasonal component is remarkably stable across years. For phosphate, the trend shows a long-term decrease over the study period, with a reduction of approximately $0.3 \mu\text{mol.L}^{-1}$ at Blainville-sur-Mer, $0.5 \mu\text{mol.L}^{-1}$ at Saint-Vaast-la-Hougue, and $0.4 \mu\text{mol.L}^{-1}$ at Utah Beach. Silicate concentrations also declined between 2000 and 2024, with reductions of $1.5 \mu\text{mol.L}^{-1}$ at Blainville-sur-Mer, $2.0 \mu\text{mol.L}^{-1}$ at Saint-Vaast-la-Hougue, and $2.5 \mu\text{mol.L}^{-1}$ at Utah Beach. The residual components for phosphate and silicate show limited short-term fluctuations, indicating the predominance of seasonal and long-term components.

Finally, although chlorophyll-a concentrations reached a minimum around 2010, this period did not coincide with minimum nutrient concentrations, suggesting asynchronous temporal dynamics.

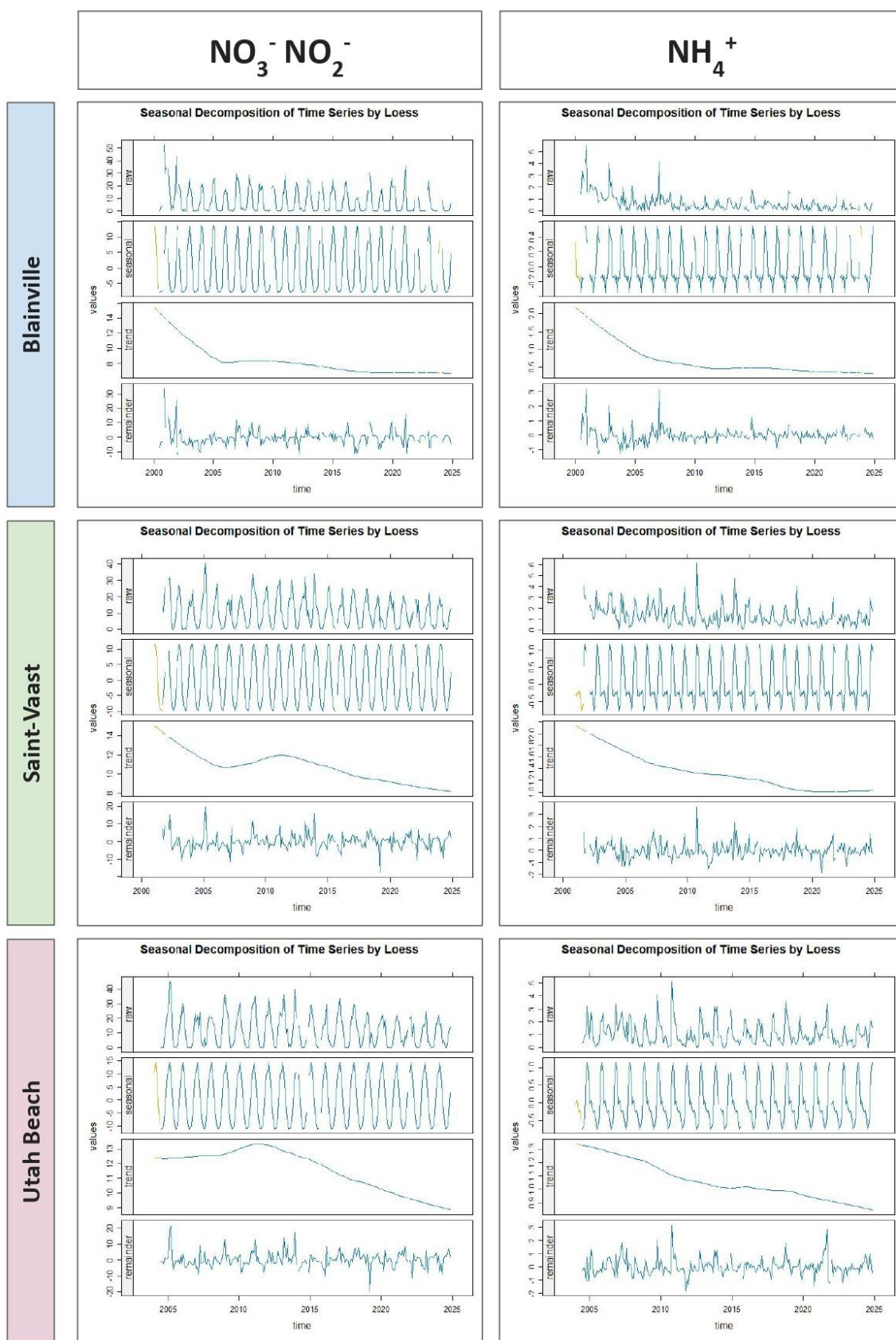
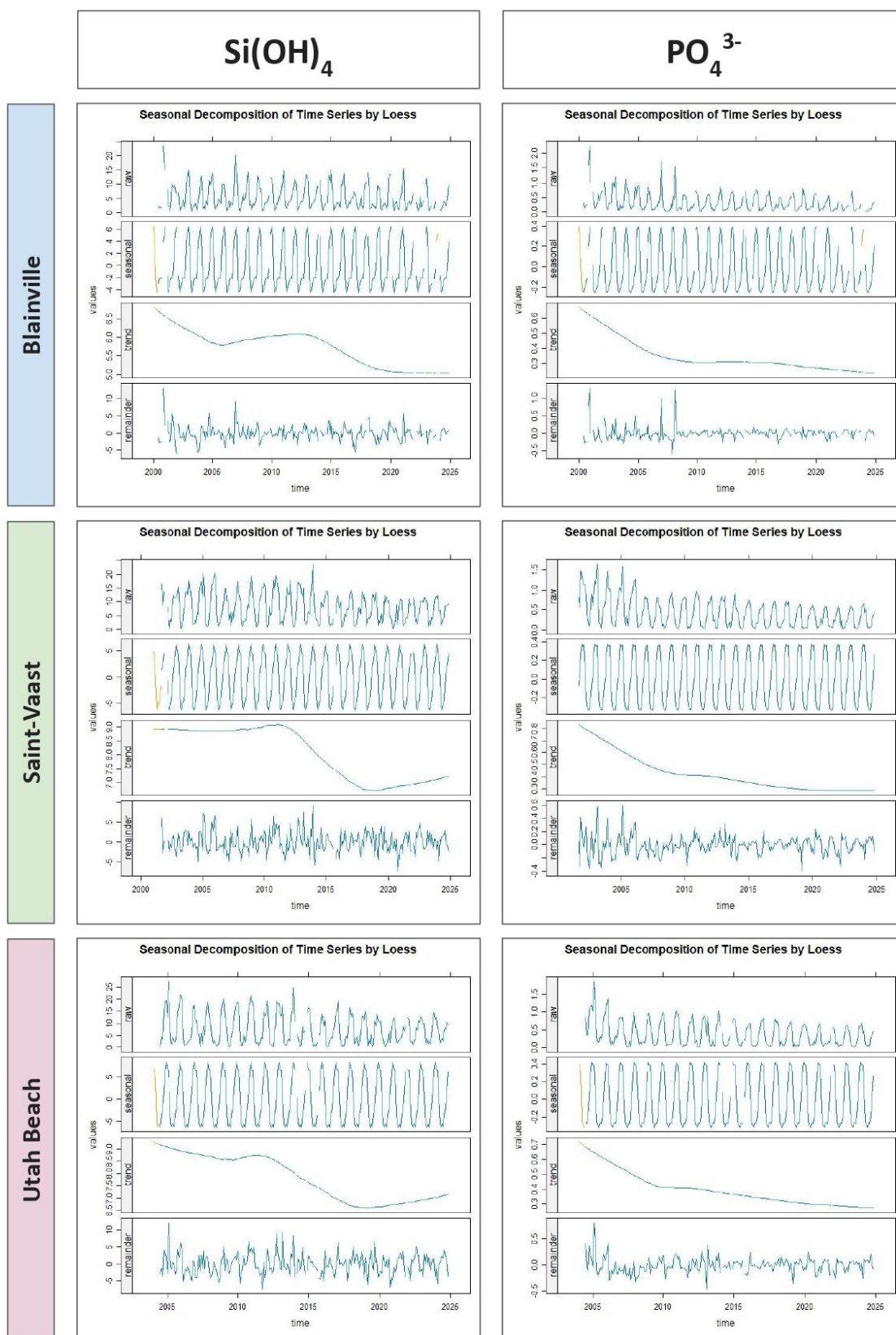


Figure 8: Seasonal decomposition of dissolved inorganic nitrogen (ammonium, nitrate, and nitrite; $\mu\text{mol L}^{-1}$) from 2000 to 2024 at the three sampling stations: Blainville-sur-Mer (blue), Saint-Vaast-la-Hougue (green), and Utah Beach (purple). For each parameter and station, four panels are shown: the original time series (*Raw*), the seasonal component (*Seasonal*), the long-term trend (*Trend*), and the residuals (*Remainder*). The decomposition was performed using LOESS smoothing with the `TrendAnalysis` function from the `TTAinterfaceTrendAnalysis` R package.



235 **Figure 9:** Seasonal Decomposition of Orthophosphate and Orthosilicic acid ($\mu\text{mol L}^{-1}$) from 2000 to 2024 at Blainville-sur-Mer, Saint-Vaast-la-Hougue, and Utah Beach. For each parameter and station, four panels are shown: the original time series (*Raw*), the seasonal component (*Seasonal*), the long-term trend (*Trend*), and the residuals (*Remainder*). The decomposition was performed using LOESS smoothing with the `TrendAnalysis` function from the `TTAinterfaceTrendAnalysis` R package.

3.4. Seasonal Patterns in Environmental Data Revealed by Principal Component Analyses

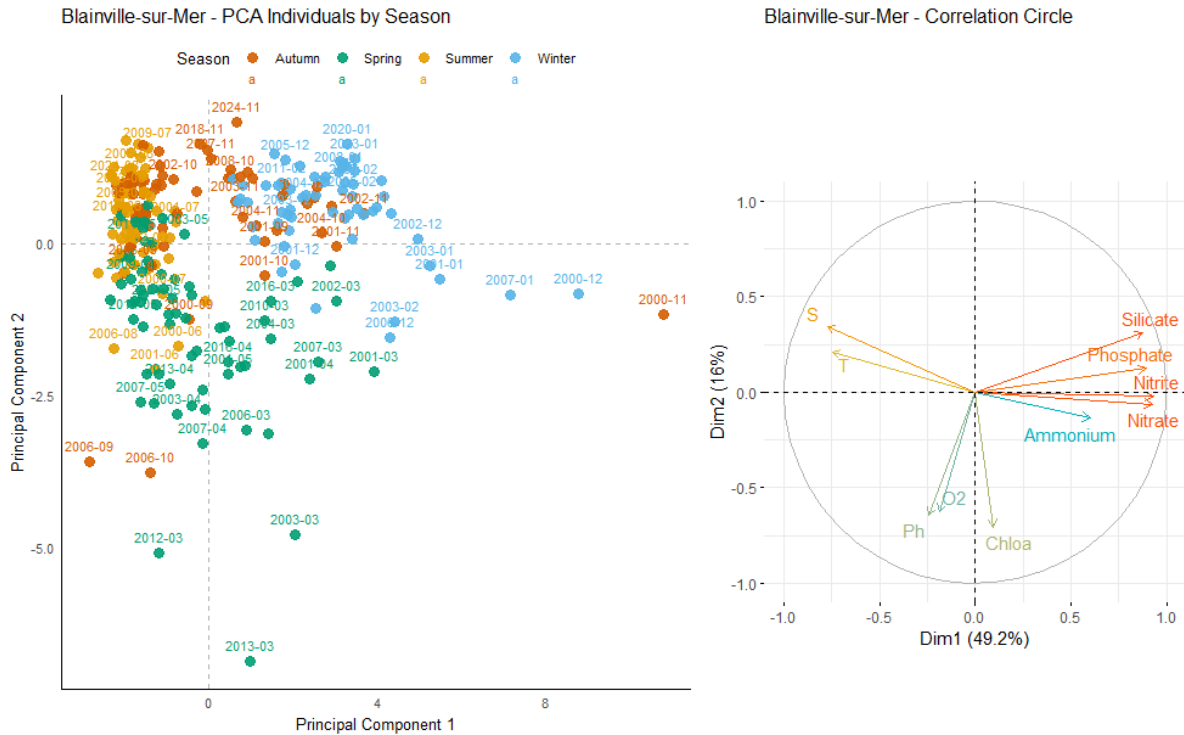


Figure 10: Principal Component Analysis of seasonal variability in physicochemical parameters and dissolved nutrients at Blainville-sur-Mer. Left: Projection of sampling dates (2000–2024) on the first two principal components. Samples are colored by season: blue (winter), green (spring), yellow (summer), and orange (autumn). Right: Correlation circle showing the contribution of environmental variables: nutrients (nitrate, nitrite, ammonium, phosphate, silicate), dissolved oxygen (O₂), pH, chlorophyll a (Chlo a), temperature (T), salinity (S).

At Blainville-sur-Mer (Figure 10), the first principal component (Dim1) explains 49.2% of the total variance, while the second component (Dim2) accounts for 16%, resulting in a cumulative variance of 65.2%. Vectors pointing to the right, which are strongly and positively correlated with Dim1, correspond to nutrient concentrations: nitrate, nitrite, phosphate, and silicate. These variables therefore explain a large part of the variability observed along Dim1. In contrast, vectors associated with dissolved oxygen, pH, and chlorophyll a point in the opposite direction, indicating a negative correlation with Dim1. Winter samples (in blue) are mostly located in the upper right quadrant of the plot, indicating an association with higher values of variables positively correlated with Dim1, such as nutrients. Conversely, spring samples (in green) tend to cluster in the lower left quadrant, suggesting an association with higher levels of dissolved oxygen (O₂), pH, and chlorophyll a (Chlo a), which are negatively correlated with Dim1. Autumn (orange) and summer (yellow) samples are more concentrated around the origin, with less dispersion. Some sampling dates appear as outliers (e.g., 2012-03, 2000-11, 2013-03), positioned at a distance from the main cluster of points.

At Saint-Vaast-la-Hougue (Figure 11), the first principal component (Dim1) explains 46.6% of the total variance, while the second component (Dim2) accounts for 21.4%. Dim1 is positively correlated with nutrient concentrations, except for ammonium, whose vector is shorter, indicating a weaker contribution to this axis.

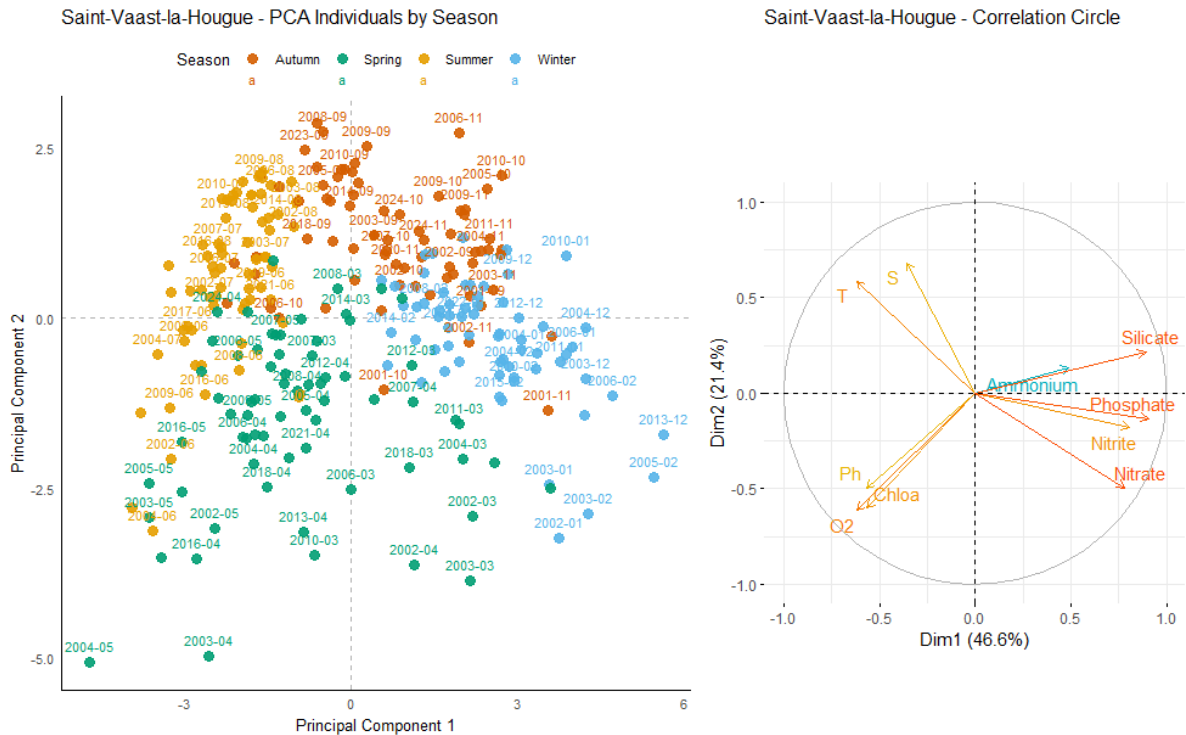


Figure 11: Principal Component Analysis of seasonal variability in physicochemical parameters and dissolved nutrients at Saint-Vaast-la-Hougue. Left: Projection of sampling dates (2000–2024) on the first two principal components. Samples are colored by season: blue (winter), green (spring), yellow (summer), and orange (autumn). Right: Correlation circle showing the contribution of environmental variables: nutrients (nitrate, nitrite, ammonium, phosphate, silicate), dissolved oxygen (O₂), pH, chlorophyll *a* (Chlo *a*), temperature (T), salinity (S).

The different seasons, represented by four distinct colors, form well-defined clusters. Blue points (winter months) are positively correlated with Dim1, whereas yellow points (summer months) are negatively correlated with this component. Green points (spring months) are located in the area associated with positive correlations to chlorophyll *a* and dissolved oxygen. Some overlap between seasons is observed, although seasonal clustering remains generally well structured.

At Utah Beach (Figure 12), the first principal component (Dim1) explains 54.5% of the total variance. It is positively correlated with nutrient concentrations such as nitrate, nitrite, phosphate, and silicate. Ammonium, shown in blue in the correlation circle, exhibits a weaker correlation with this component. Temperature, salinity, dissolved oxygen, and chlorophyll *a* are negatively correlated with Dim1. The second component (Dim2) accounts for 17.4% of the variance.

Winter observations (blue) are primarily located on the right-hand side of Dim1, associated with positive values and higher nutrient concentrations. In contrast, summer observations (yellow) tend to cluster on the left-hand side, where nutrient levels are lower. Spring samples (green) occupy an intermediate position, with some overlap, in the area associated with chlorophyll *a* and dissolved oxygen.

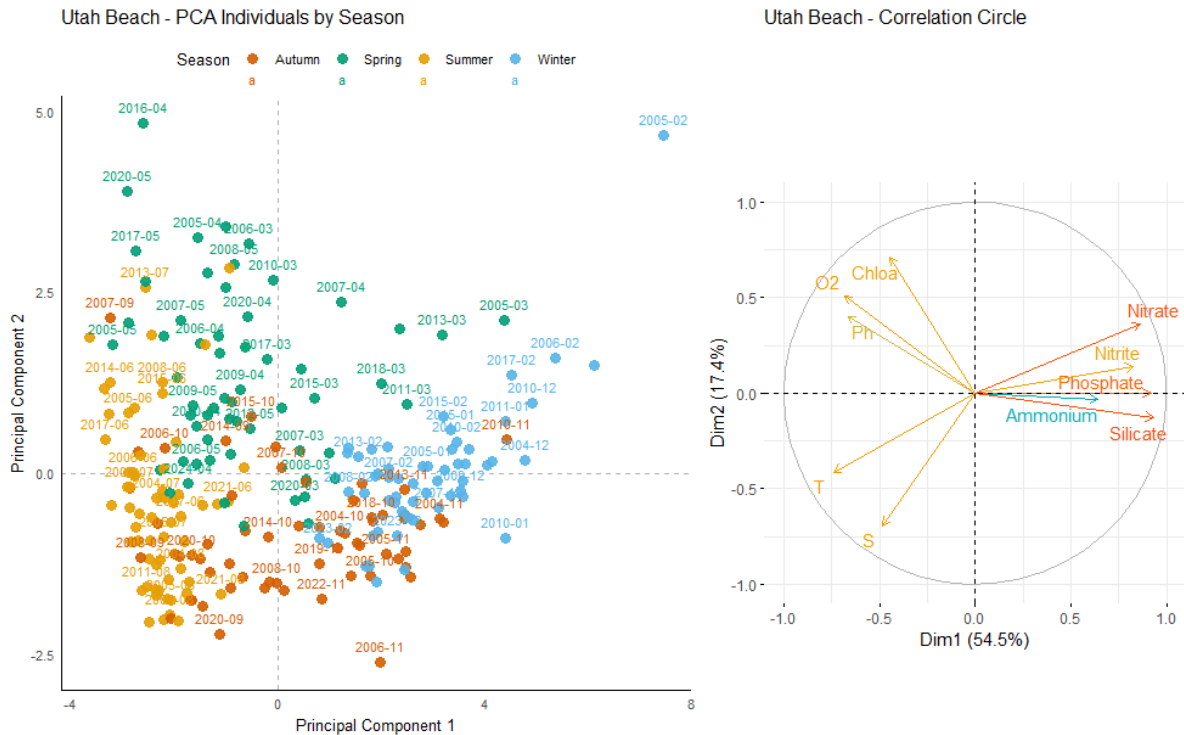


Figure 12: Principal Component Analysis of seasonal variability in physicochemical parameters and dissolved nutrients at Utah Beach. Left: Projection of sampling dates (2000–2024) on the first two principal components. Samples are colored by season: blue (winter), green (spring), yellow (summer), and orange (autumn). Right: Correlation circle showing the contribution of environmental variables: nutrients (nitrate, nitrite, ammonium, phosphate, silicate), dissolved oxygen (O₂), pH, chlorophyll a (Chlo a), temperature (T), salinity (S).

3.5. Stoichiometric Limitations

The variations in macronutrient concentrations described in [Figure 6](#) influenced the stoichiometric ratios. Data aggregated from 2000 to 2024 reveal two distinct nutrient limitation dynamics depending on the coastline. At Blainville-sur-Mer, nitrogen was identified as the primary limiting nutrient in 186 observations, followed by silica (101 observations), while phosphorus was least frequently limiting (100 observations) ([Table 3](#)). On the eastern coast, phosphorus appeared most frequently as the limiting nutrient, with 185 observations at Saint-Vaast-la-Hougue and 182 at Utah Beach. In both of these stations, silica and nitrogen were less frequently limiting, with 107 and 95 observations for silica at Saint-Vaast-la-Hougue and Utah Beach, respectively, and 90 and 75 for nitrogen. These distributions are consistent with the classification shown in [Figure 13](#), which groups observations into six categories based on the relative order of nutrient limitation. Notably, the nutrient limitation patterns at Saint-Vaast-la-Hougue and Utah Beach are highly similar, with only slight differences in the relative frequencies of the $P < Si < N$ and $N < Si < P$ categories.

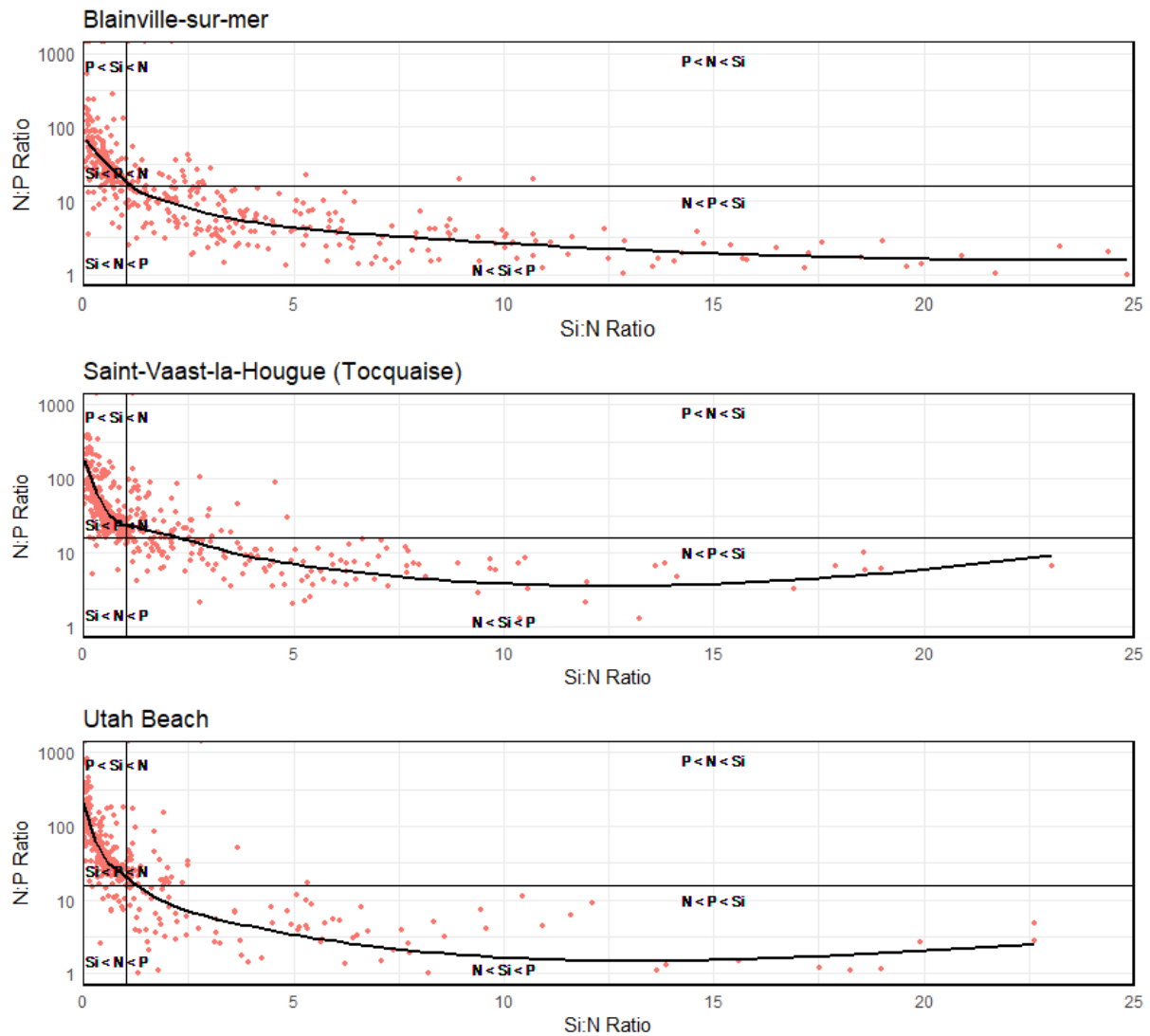


Figure 13: Synthetic graph showing the molar ratios of Si:N:P from 2000 to 2024 at Blainville-sur-Mer, Saint-Vaast-la-Hougue, and Utah Beach. The plot is divided into six regions based on stoichiometric thresholds for biogenic particles, following Redfield et al. (1963) and Brzezinski (1985) ($\text{Si:N:P} = 16:16:1$). These regions indicate the order of priority for potentially limiting nutrients in each ecosystem.

Table 3: Distribution of observations based on the potential limiting nutrient (from most to least limiting) at the three stations (Blainville-sur-Mer, Saint-Vaast-la-Hougue, and Utah Beach) from 2000 to 2024.

	Blainville-sur-mer	Saint-Vaast-la-Hougue	Utah Beach	Total
P<Si<N	100	185	182	467
Si<P<N	101	107	95	303
N<Si<P	186	90	75	351
N<P<Si	48	41	34	123
Si<N<P	19	8	15	42
<i>n</i>	454	431	401	1286

4. Discussion

The results of this study highlight the importance of conducting long-term monitoring at specific sites to better understand intra- and inter-annual variations in the biogeochemical cycles of nutrients and the evolution of physico-chemical parameters.

4.1. Data Quality and Limitations

The dataset compiled for this study is based on consistent sampling and analytical protocols applied from 2000 to 2024 across three coastal stations in Normandy. Sampling was conducted bi-monthly under standardized conditions, and nutrient analyses followed validated spectrophotometric methods in accordance with French and international standards (*e.g.*, AFNOR XP T90-210). Quality assurance procedures included daily calibration of instruments, use of certified reference materials, and strict control over sample storage and processing times to limit degradation. Detection and quantification limits were determined for each parameter and are provided in [Table 2](#) to support the interpretation of low-concentration values.

Despite the methodological rigor, some limitations should be acknowledged. Occasional data gaps are present, primarily due to adverse weather conditions or logistical constraints. Moreover, while the protocols ensure a high degree of comparability over time, analytical sensitivity may have evolved slightly over the 24-year period due to changes in equipment and detection capabilities. Finally, although extreme outliers were rare and handled using robust statistical methods, a small number of values were excluded following established quality control criteria. Overall, the dataset is considered highly reliable for assessing long-term stoichiometric trends and nutrient limitation patterns in the studied ecosystems

4.2. Coastal Ecosystems and Climate Change

The three studied sites, located in the Normandy region, show a progressive increase in winter temperatures over the past decade ([Figure 2](#), [Figure 3](#)). This finding aligns with observations made at other monitoring points in the English Channel ([Cornes *et al.*, 2023](#) ; [Kassem & Thompson, 2023](#) ; [McEvoy *et al.*, 2023](#) ; [Hubert *et al.*, 2024](#) ; [Neven *et al.*, 2024](#)). While our data indicate an average rise of 1°C over 12 years for the three stations, studies conducted along the southern coast of England report an increase ranging from 0.42°C to 0.76°C per decade ([Kassem & Thompson, 2023](#)). In France, [Hubert *et al.* \(2024\)](#) reported a similar warming trend, estimated at +1.063°C over 11 years. Moreover, the year 2022 was marked by an exceptional heatwave, recorded by [Simon *et al.* \(2023\)](#), with particularly high summer temperatures ([Guinaldo *et al.*, 2023](#) ; [Hubert *et al.*, 2024](#)). This phenomenon was also observed within our monitoring network. However, natural temperature oscillations, such as the Atlantic Multidecadal Oscillation (AMO; [Kerr, 2000](#)), also affect conditions in the English Channel ([Edwards *et al.*, 2013](#) ; [Auber *et al.*, 2017](#)).

The warming of coastal waters may lead to significant changes in marine ecosystems, particularly by altering the composition and biomass of phytoplankton communities ([Richardson & Schoeman, 2004](#)), zooplankton ([Neven *et al.*, 2024](#)), and fish populations ([Auber *et al.*, 2017](#) ; [Maltby *et al.*, 2020](#)). These changes could have major repercussions on the dynamics of coastal ecosystems and the services they provide. Another

major factor threatening marine ecosystems is ocean acidification. Observations and modeling studies indicate a global decrease in ocean pH by 0.02 units per decade, with a projected drop of up to -0.7 units by 2100 due to the dissolution of atmospheric CO₂ into the oceans ([Calderira & Wickett, 2003](#) ; [Bates, 2007](#) ; [Santana *et al.*, 2007](#) ; [Olafsson *et al.*, 2009](#) ; [Lauvset *et al.*, 2016](#)). Such acidification will have significant consequences, including altering the structure of marine communities ([Fabry *et al.*, 2008](#)), disrupting nutrient cycles ([Hutchins *et al.*, 2009](#)), reducing productivity ([Riebesell *et al.*, 2007](#)), and impacting carbon fluxes ([Schulz *et al.*, 2008](#)).

Data from the HYDRONOR observatory reveal an average acidification over 24 years of -0.2 units in Blainville-sur-Mer, -0.25 units in Saint-Vaast-la-Hougue, and -0.15 units in Utah Beach. These values significantly exceed previously predicted levels, highlighting the urgency of better understanding these phenomena. Long-term monitoring of coastal ecosystems is crucial to understanding the effects of climate change, particularly in shellfish farming areas where bivalves, vulnerable due to their calcareous shells, are heavily impacted by acidification ([Doney *et al.*, 2020](#)). However, coastal zones present specific challenges due to their high daily, seasonal, and interannual variability. This complexity, influenced by factors such as riverine inputs, climatic conditions, and anthropogenic pressures, makes identifying climate change-related trends more difficult ([Kapsenberg *et al.*, 2017](#); [Reimer *et al.*, 2017](#) ; [Chen & Hu, 2019](#)).

4.3. Ecological Contrasts between the West and East Coasts of Cotentin

Our findings highlight two distinct ecological dynamics between the West and East coasts of Cotentin. The West coast, represented by the Blainville-sur-Mer station, is characterized by an open environment where processes appear to "dilute," leading to consistent and regular seasonal trends. As shown in [Figure 4](#), chlorophyll *a* peaks occur systematically in March, with variations mainly limited to the amplitude of phytoplankton blooms. In contrast, the East coast exhibits much less predictable and highly variable trends from year to year. Regarding dissolved nutrients, although maximum concentrations are similar between the two coasts (except for ammonium, [Figure 6](#)), these peaks are short-lived on the West coast.

We hypothesize that this "dilution" of processes on the West coast is linked to its open environment, with greater exchange with the English Channel and the Atlantic Ocean. Conversely, the East coast, influenced by the proximity of bays and riverine inputs ([Figure 1](#)), experiences more intense and irregular phenomena. A notable difference lies in the limiting elements: the West coast is primarily nitrogen-deficient, whereas the East coast is limited by phosphorus and silica ([Figure 13](#)). These observations contrast with studies conducted in the English Channel, which generally report a nitrogen surplus due to agricultural activities and riverine inputs ([Ménèsqueun *et al.*, 2019](#) ; [Romero *et al.*, 2019](#) ; [Yan *et al.*, 2021](#) ; [Yan *et al.*, 2022](#)).

The PCA results ([Figures 10, 11 and 12](#)) support and further illustrate these contrasting ecological dynamics. At Blainville-sur-Mer (West coast, [Figure 10](#)), the seasonal structure appears particularly regular and well-defined. The PCA shows a clear separation of winter and spring samples along the first principal component (Dim1), primarily driven by nutrient concentrations and their inverse relationship with temperature, salinity, and biological activity indicators such as chlorophyll *a* and dissolved oxygen. This regular structure aligns with the hypothesis of a diluted, open system dominated by predictable seasonal patterns and nutrient cycling. In contrast, at Saint-Vaast-la-Hougue and Utah Beach (East coast, [Figures 11 and 12](#)), the PCA reveals greater seasonal dispersion and overlap, especially in spring and summer, indicating more variable and less predictable environmental conditions. These stations show a more complex multivariate structure, with spring samples, in

particular, spreading across both axes, reflecting the influence of both nutrient enrichment and variable biological responses. The position of ammonium, weakly correlated with Dim1 at both East coast stations, suggests localized, irregular inputs, possibly linked to anthropogenic or benthic sources. Moreover, the nutrient vectors in the correlation circles are generally longer and more dominant in the East coast stations, especially at Saint-Vaast, suggesting that nutrient variability plays a stronger role in structuring the ecosystem in these areas. This supports the idea of more intense, irregular phenomena on the East coast, likely influenced by confined hydrodynamics, river discharges, and bay retention.

Differences between the ecosystems of the East and West coasts of the Cotentin Peninsula have already been highlighted in previous studies. Lefebvre et al. (2009a ; 2009b) found that the diet of oysters on the West coast was primarily based on phytoplankton (*i.e.*, pelagic), whereas on the East coast, the animals consumed a mix of benthic and pelagic sources.

4.4. Drivers of Long-Term Nutrient Decline in Coastal Waters

Since the 1980s, European policies have aimed to reduce nutrient inputs, particularly phosphates and nitrates, from agricultural sources (Claussen et al., 2009 ; Garnier et al., 2019). Long-term analyses confirm that phytoplankton biomass is closely linked to both nutrient availability and hydroclimatic conditions (Loebl et al., 2009). Over the study period, a general decrease in dissolved nutrient concentrations - including ammonium, nitrate, nitrite, phosphate, and silicate—was observed across all three stations (Figures 8 and 9). This reduction coincides with a widespread decline in chlorophyll *a* concentrations since the early 2000s (Goberville et al., 2010 ; Gohin et al., 2019), as illustrated in Figure 7.

The decline in nitrogen and phosphorus concentrations is consistent with the implementation of agricultural regulations, including fertilizer use restrictions and wastewater treatment improvements (Claussen et al., 2009 ; Garnier et al., 2019). However, silicate is not directly influenced by such human inputs, as it mainly originates from the chemical weathering of continental rocks and is transported to the coastal zone via river discharge (Nelson & Gordon, 1982 ; Tréguer & De La Rocha, 2013).

The observed decrease in silicate concentrations therefore suggests a reduction in freshwater inflows to the coastal zone, potentially linked to lower river discharge. While hydrological data are sparse at the local scale, national assessments by ONEMA (Giuntoli et al., 2012) indicate that no significant trends in annual mean flows were detected in northern France between 1968 and 2007, in contrast to marked decreases in southern regions. However, recent climate trends - including increased evapotranspiration, altered precipitation patterns, and higher interannual variability - could still result in seasonal or event-scale reductions in riverine inputs to the coastal zone, which may not be captured by annual averages (Collet et al., 2014 ; Mimeau et al., 2025).

Additionally, anthropogenic alterations to watersheds, such as damming and land-use changes, have been shown to impact the silicon cycle by reducing dissolved silica export to estuaries (Ittekkot et al., 2006 ; Laruelle et al., 2009 ; Bernard et al., 2011). These changes, combined with climate-driven alterations in hydrology (Bernard et al., 2010), suggest that the silicon cycle in coastal ecosystems is highly sensitive to both direct human modification and indirect climate forcing, potentially affecting diatom-based primary production and broader food web dynamics.

5. Conclusion

This study provides valuable insights into the long-term trends of hydrobiological parameters in Normandy's shellfish ecosystems, emphasizing the significant impacts of both human activity and climate change. Our analysis highlights a consistent increase in winter temperatures and a gradual acidification of pH levels across all three monitoring stations (Blainville-sur-Mer, Saint-Vaast-la-Hougue, and Utah Beach) from 2000 to 2024. These changes align with broader trends observed in the English Channel and suggest a shift in the environmental conditions that could affect the ecological balance of coastal habitats.

The observed variations in chlorophyll *a* concentrations and nutrient dynamics reveal complex interactions between nutrient availability, primary production, and the potential limitations of different nutrients across seasons. Notably, nitrogen was identified as the primary limiting nutrient in the western region, while phosphorus dominated as the limiting factor in the eastern stations. These findings have important implications for managing nutrient inputs and maintaining the health of coastal ecosystems, particularly in the context of ongoing eutrophication.

Furthermore, the study underscores the importance of sustained, site-specific monitoring to capture the intricate and evolving dynamics of coastal environments. The long-term dataset from the HYDRONOR observatory has proven essential in understanding how climatic shifts, such as increased temperatures, influence phytoplankton blooms and nutrient cycling. This research provides a crucial foundation for future efforts to mitigate the impacts of climate change and anthropogenic pressures on coastal ecosystems, particularly those supporting critical industries like shellfish farming. As the region faces rising temperatures and ongoing nutrient imbalances, adaptive management strategies will be key to preserving the resilience of these vital ecosystems.

6. Data and code availability

The hydrobiological dataset from the HYDRONOR Observatory is openly accessible on Zenodo at the following DOI: <https://doi.org/10.5281/zenodo.15058835> (SMEL - Synergie Mer & Littoral, 2024). Additionally, the R package **TTAinterfaceTrendAnalysis**, designed for trend analysis, is available for consultation and download directly from the CRAN website: <https://cran.r-project.org/web/packages/TTAinterfaceTrendAnalysis/index.html>.

7. Author contribution

JS wrote the paper. JB and SP coordinate the ecological monitoring of the HYDRONOR observatory. SP developed all the methodologies and has conducted all laboratory analyses since 2000.

8. Competing interests

The authors declare that they have no conflict of interest.

9. Acknowledgements

We express our gratitude to all the SMEL agents who have contributed to hydrobiological monitoring over the years through their dedicated efforts in data collection and fieldwork.

10. Financial support

This study was supported by the HYDRONOR observatory, which is funded by SMEL's own resources (Departmental Council of Manche, CD50).

11. References

- Aminot, A., & Chaussepied, M. (1983). *Manuel des analyses chimiques en milieu marin*. Ifremer.
- Aminot, A., & K  rouel, R. (2004). *Hydrologie des   cosyst  mes marins : param  tres et analyses*.   ditions Quae.
- Auber, A., Gohin, F., Goascoz, N., & Schlaich, I. (2017). Decline of cold-water fish species in the Bay of Somme (English Channel, France) in response to ocean warming. *Estuarine, Coastal and Shelf Science*, 189, 189–202. <https://doi.org/10.1016/j.ecss.2017.03.004>
- Barbier, E. B., Hacker, S. D., Kennedy, C., Koch, E. W., Stier, A. C., & Silliman, B. R. (2011). The value of estuarine and coastal ecosystem services. *Ecological Monographs*, 81(2), 169–193. <https://doi.org/10.1890/10-1510.1>
- Bates, N. R. (2007). Interannual variability of the oceanic CO₂ sink in the subtropical gyre of the North Atlantic Ocean over the last 2 decades. *Journal of Geophysical Research: Oceans*, 112, C09013. <https://doi.org/10.1029/2006JC003759>
- Beaugrand, G. (2004). Monitoring marine plankton ecosystems. I: Description of an ecosystem approach based on plankton indicators. *Marine Ecology Progress Series*, 269, 69–81. <https://doi.org/10.3354/meps269069>
- Bendschneider, K., & Robinson, R. J. (1952). A new spectrophotometric method for the determination of nitrite in sea water. *Journal of Marine Research*, 11, 87–96.
- Bernard, C. Y., Durr, H. H., Heinze, C., Segschneider, J., & Meier-Reimer, E. (2011). Contribution of riverine nutrients to the silicon biogeochemistry in the global ocean—a model study. *Biogeosciences*, 8, 551–564. <https://doi.org/10.5194/bg-8-551-2011>
- Bernard, C. Y., Laruelle, G. G., Slomp, C. P., & Heinze, C. (2010). Impact of changes in river fluxes of silica on the global marine silicon cycle: A model comparison. *Biogeosciences*, 7, 441–453. <https://doi.org/10.5194/bg-7-441-2010>
- Brzezinski, M. A. (1985). The Si:C:N ratio of marine diatoms: Interspecific variability and the effect of some environmental variables. *Journal of Phycology*, 21, 347–357. <https://doi.org/10.1111/j.0022-3646.1985.00347.x>
- Cad  e, G. C., & Hegeman, J. (2002). Phytoplankton in the Marsdiep at the end of the 20th century: 30 years monitoring biomass, primary production, and *Phaeocystis* blooms. *Journal of Sea Research*, 48(2), 97–110. [https://doi.org/10.1016/S1385-1101\(02\)00161-0](https://doi.org/10.1016/S1385-1101(02)00161-0)
- Caldeira, K., & Wickett, M. E. (2003). Anthropogenic carbon and ocean pH. *Nature*, 425, 365. <https://doi.org/10.1038/425365a>
- Chen, S., & Hu, C. (2019). Environmental controls of surface water pCO₂ in different coastal environments: Observations from marine buoys. *Continental Shelf Research*, 183, 73–86. <https://doi.org/10.1016/j.csr.2019.05.007>
- Chenel, J. (2025). *  tude du compartiment « chimie » du projet CarUtah* (Master's thesis). Synergie Mer et Littoral (SMEL).

- Claussen, U., Zevenboom, W., Brockmann, U., Topcu, D., & Bot, P.** (2009). Assessment of the eutrophication status of transitional, coastal and marine waters within OSPAR. *Hydrobiologia*, 629, 49–58. <https://doi.org/10.1007/s10750-009-9763-3>
- 505 **Cloern, J. E.** (2001). Our evolving conceptual model of the coastal eutrophication problem. *Marine Ecology Progress Series*, 210, 223–253. <https://doi.org/10.3354/meps210223>
- Collet, L., Ruelland, D., Borrell-Estupina, V., & Servat, E.** (2014). Variabilité climatique et des activités humaines sur les ressources en eau d'un bassin Méditerranéen de méso-échelle. *Hydrological Sciences Journal*, 59(8), 1457–1469. <https://doi.org/10.1080/02626667.2013.842073>
- 510 **Cornes, R. C., Tinker, J., Hermanson, L., Oltmanns, M., Hunter, W. R., Lloyd-Hartley, H., Kent, E. C., Rabe, B., & Renshaw, R.** (2023). *The impacts of climate change on sea temperature around the UK and Ireland* (18 pp.). Marine Climate Change Impacts Partnership.
- Devreker, D., & Lefebvre, A.** (2014). TTAinterfaceTrendAnalysis: A R GUI for routine temporal trend analysis and diagnostics. *Journal of Oceanography, Research and Data*, 6, 1–18.
- 515 **Diaz, R. J.** (2001). Overview of hypoxia around the world. *Journal of Environmental Quality*, 30, 275–281. <https://doi.org/10.2134/jeq2001.302275x>
- Doney, S. C., Busch, D. S., Cooley, S. R., & Kroeker, K. J.** (2020). The impacts of ocean acidification on marine ecosystems and reliant human communities. *Annual Review of Environment and Resources*, 45, 83–112. <https://doi.org/10.1146/annurev-environ-012320-083019>
- 520 **Dudgeon, D., Arthington, A. H., Gessner, M. O., Kawabata, Z. I., Knowler, D. J., Lévêque, C., Naiman, R. J., Prieur-Richard, A. H., Soto, D., Stiassny, M. L. J., & Sullivan, C. A.** (2006). Freshwater biodiversity: Importance, threats, status and conservation challenges. *Biological Reviews*, 81, 163–182. <https://doi.org/10.1017/S1464793105006950>
- Edwards, M., Beaugrand, G., Helaouët, P., Alheit, J., & Coombs, S.** (2013). Marine ecosystem response to the Atlantic Multidecadal Oscillation. *PLOS ONE*, 8(2), e57212. <https://doi.org/10.1371/journal.pone.0057212>
- 525 **Fabry, V. J., Seibel, B. A., Feely, R. A., & Orr, J. C.** (2008). Impacts of ocean acidification on marine fauna and ecosystem processes. *ICES Journal of Marine Science*, 65(3), 414–432. <https://doi.org/10.1093/icesjms/fsn048>
- 530 **Filgueira, R., Guyondet, T., Comeau, L. A., & Tremblay, R.** (2016). Bivalve aquaculture–environment interactions in the context of climate change. *Global Change Biology*, 22(12), 3901–3913. <https://doi.org/10.1111/gcb.13346>
- Garnier, J., Riou, P., Le Gendre, R., Ramarson, A., Billen, G., Cugier, P., Schapira, M., Thery, S., Thieu, V., & Menesguen, A.** (2019). Managing the agri-food system of watersheds to combat coastal eutrophication: A land-to-sea modelling approach to the French Coastal English Channel. *Geosciences*, 9, 441. <https://doi.org/10.3390/geosciences9100441>
- 535

Giuntoli, I., Maugis, P., & Renard, B. (2012). *Évolutions observées dans les débits des rivières en France : Sélection d'un réseau de référence et analyse de l'évolution temporelle des régimes des 40 dernières années* (8 p.). Onema. Collection « Comprendre pour agir ».

540 **Goberville, E., Beaugrand, G., Sautour, B., Tréguer, P., & Somelit team.** (2010). Climate-driven changes in coastal marine systems of western Europe. *Marine Ecology Progress Series*, 408, 129–147. <https://doi.org/10.3354/meps08564>

Gohin, F., Van der Zande, D., Tilstone, G., Eleveld, M. A., Lefebvre, A., Andrieux-Loyer, F., Blauw, A. N., Bryère, P., Devreker, D., Garnesson, P., Hernandez Farinas, T., Lamaury, Y., Lampert, L.,
545 **Lavigne, H., Menet-Nedelec, F., Pardo, S., & Saulquin, B.** (2019). Twenty years of satellite and in situ observations of surface chlorophyll-a from the northern Bay of Biscay to the eastern English Channel. Is the water quality improving? *Remote Sensing of Environment*, 233, 111343. <https://doi.org/10.1016/j.rse.2019.111343>

Grangere, K. (2004). *Simulation de l'influence des apports des bassins versants sur les concessions ostréicoles de la Baie des Veys (Baie de Seine Occidentale)* [Post-graduate thesis (DEA), University of Caen].
550

Guinaldo, T., Voldoire, A., Waldman, R., Saux Picart, S., & Roquet, H. (2023). Response of the sea surface temperature to heatwaves during the France 2022 meteorological summer. *Ocean Science*, 19(3), 629–647. <https://doi.org/10.5194/os-19-629-2023>

Halpern, B. S., Selkoe, K. A., Micheli, F., & Kappel, C. V. (2007). Evaluating and ranking the vulnerability of global marine ecosystems to anthropogenic threats. *Conservation Biology*, 21, 1301–1315. <https://doi.org/10.1111/j.1523-1739.2007.00752.x>
555

Heisler, J., Glibert, P. M., Burkholder, J. M., Anderson, D. M., Cochlan, W., Dennison, W. C., Dortch, Q., Gobler, C. J., Heil, C. A., Humphries, E., Lewitus, A., Magnien, R., Marshall, H. G., Sellner, K., Stockwell, D. A., Stoecker, D. K., & Suddleson, M. (2008). Eutrophication and harmful algal blooms:
560 A scientific consensus. *Harmful Algae*, 8(1), 3–13. <https://doi.org/10.1016/j.hal.2008.08.006>

Hubert, Z., Louchart, A., Robache, K., Epinoux, A., Gallot, C., Cornille, V., Crouvoisier, M., Monchy, S., & Artigas, L. F. (2024). Decadal changes in phytoplankton functional composition in the Eastern English Channel: Evidence of upcoming major effects of climate change? *EGUsphere*, 2024, 1–28. <https://doi.org/10.5194/egusphere-2024-222>

565 **Hutchins, D. A., Mulholland, M. R., & Fu, F.** (2009). Nutrient cycles and marine microbes in a CO₂-enriched ocean. *Oceanography*, 22(4), 128–145. <https://doi.org/10.5670/oceanog.2009.103>

Ittekkot, V., Unger, D., Humborg, C., & An, N. T. (Eds.). (2006). *The silicon cycle: Human perturbations and impacts on aquatic systems* (SCOPE Series Vol. 66, 296 pp.). Island Press.

Kapsenberg, L., Alliouane, S., Gazeau, F., Mousseau, L., & Gattuso, J.-P. (2017). Coastal ocean acidification and increasing total alkalinity in the northwestern Mediterranean Sea. *Ocean Science*, 13, 411–426. <https://doi.org/10.5194/os-13-411-2017>
570

- Kassem, H., Amos, C. L., & Thompson, C. E. L.** (2023). Sea surface temperature trends in the coastal zone of southern England. *Journal of Coastal Research*, 39(1), 18–31. <https://doi.org/10.2112/JCOASTRES-D-22-00056.1>
- 575 **Kerr, R. A.** (2000). A North Atlantic climate pacemaker for the centuries. *Science*, 288(5473), 1984–1985. <https://doi.org/10.1126/science.288.5473.1984>
- Kirby, R., Beaugrand, G., & Lindley, J. A.** (2009). Synergistic effects of climate and fishing in a marine ecosystem. *Ecosystems*, 12, 548–561. <https://doi.org/10.1007/s10021-009-9241-9>
- Laruelle, G. G., Roubéix, V., Sferratore, A., Brodherr, B., Ciuffa, D.** (2009). Anthropogenic perturbations of the silicon cycle at the global scale: Key role of the land-ocean transition. *Global Biogeochemical Cycles*, 23, GB4031. <https://doi.org/10.1029/2008GB003267>
- 580 **Lauvset, S. K., Key, R. M., Olsen, A., van Heuven, S., Velo, A., Lin, X., Schirnick, C., Kozyr, A., Tanhua, T., Hoppema, M., Jutterström, S., Steinfeldt, R., Jeansson, E., Ishii, M., Pérez, F. F., Suzuki, T., & Watelet, S.** (2016). A new global interior ocean mapped climatology: The 1×1 GLODAP version 2. *Earth System Science Data*, 8, 325–340. <https://doi.org/10.5194/essd-8-325-2016>
- 585 **Lefebvre, A., Guiselin, N., Barbet, F., & Artigas, L. F.** (2011). Long-term hydrological and phytoplankton monitoring (1992–2007) of three potentially eutrophicated systems in the eastern English Channel and the southern bight of the North Sea. *ICES Journal of Marine Science*, 68(10), 2029–2043. <https://doi.org/10.1093/icesjms/fsr151>
- 590 **Lefebvre, S., Harma, C., & Blin, J. L.** (2009b). Trophic typology of coastal ecosystems based on $\delta^{13}\text{C}$ and $\delta^{15}\text{N}$ ratios in an opportunistic suspension feeder. *Marine Ecology Progress Series*, 390, 27–37. <https://doi.org/10.3354/meps08170>
- Lefebvre, S., Marín Leal, J. C., Dubois, S., Orvain, F., Blin, J. L., Bataillé, M. P., Ourry, A., & Galois, R.** (2009a). Seasonal dynamics of trophic relationships among co-occurring suspension feeders in two shellfish culture dominated ecosystems. *Estuarine, Coastal and Shelf Science*, 82, 415–425. <https://doi.org/10.1016/j.ecss.2009.02.026>
- 595 **Leruste, A., Pasqualini, V., Garrido, M., Malet, N., De Wit, R., & Bec, B.** (2019). Physiological and behavioral responses of phytoplankton communities to nutrient availability in a disturbed Mediterranean coastal lagoon. *Estuarine, Coastal and Shelf Science*, 219, 176–188. <https://doi.org/10.1016/j.ecss.2019.01.009>
- 600 **Loebl, M., Colijn, F., van Beusekom, J. E. E., Baretta-Bekker, J. G., Lancelot, C., Philippart, C. J. M., Rousseau, V., & Wiltshire, K. H.** (2009). Recent patterns in potential limitation along the Northwest European continental coast. *Journal of Sea Research*, 61, 34–43. <https://doi.org/10.1016/j.seares.2008.05.002>
- Maltby, K. M., Rutterford, L. A., Tinker, J., Genner, M. J., & Simpson, S. D.** (2020). Projected impacts of warming seas on commercially fished species at a biogeographic boundary of the European continental shelf. *Journal of Applied Ecology*, 57(11), 2222–2233. <https://doi.org/10.1111/1365-2664.13682>
- 605 **Martin, G. D., Vijay, J. G., Laluraj, C. M., Madhu, N. V., Joseph, T., Nair, M., Gupta, G. V. M., & Balachandran, K. K.** (2008). Fresh water influence on nutrient stoichiometry in a tropical estuary,

southwest coast of India. *Applied Ecology and Environmental Research*, 6, 57–64.
https://doi.org/10.15666/aeer/0601_057064

McEvoy, A. J., Atkinson, A., Airs, R. L., Brittain, R., Brown, I., Fileman, E. S., Findlay, H. S., McNeil, C. L., Ostle, C., Smyth, T. K., Somerfield, P. J., Tait, K., Tarran, G. A., Thomas, S., Widdicombe, C. E., Woodward, E., Beesley, A., Conway, D. V. P., Fishwick, J., Widdicombe, S. (2023). The Western Channel Observatory: A century of physical, chemical and biological data compiled from pelagic and benthic habitats in the western English Channel. *Earth System Science Data*, 15(12), 5701–5737.
<https://doi.org/10.5194/essd-15-5701-2023>

Ménesguen, A., Dussauze, M., Dumas, F., Thouvenin, B., Garnier, V., Lecornu, F., & Répécaud, M. (2019). Ecological model of the Bay of Biscay and English Channel shelf for environmental status assessment. Part 1: Nutrients, phytoplankton and oxygen. *Ocean Modelling*, 133, 56–78.
<https://doi.org/10.1016/j.ocemod.2018.11.005>

Meybeck, M., Lestel, L., Carré, C., Bouleau, G., Garnier, J., & Mouchel, J. M. (2018). Trajectories of river chemical quality issues over the longue durée: The Seine River (1900s–2010). *Environmental Science and Pollution Research*, 25, 23468–23484.

Mimeau, L., Künné, A., Devers, A., Branger, F., Kralisch, S., Lauvernet, C., Vidal, J.-P., Bonada, N., Csabai, Z., Mykrä, H., Pařil, P., Polović, L., & Datry, T. (2025). Projections of streamflow intermittence under climate change in European drying river networks. *Hydrology and Earth System Sciences*, 29(6), 1615–1636. <https://doi.org/10.5194/hess-29-1615-2025>

Mullin, J., & Riley, J. P. (1955). The colorimetric determination of silicate with special reference to sea and natural waters. *Analytica Chimica Acta*, 12, 162–176.

Murphy, J., & Riley, J. P. (1962). A modified single solution method for the determination of phosphate in natural waters. *Analytica Chimica Acta*, 27, 31–36.

Nelson, D. M., & Gordon, L. I. (1982). Production and pelagic dissolution of biogenic silica in the Southern Ocean. *Geochimica et Cosmochimica Acta*, 46, 491–501. [https://doi.org/10.1016/0016-7037\(82\)90153-3](https://doi.org/10.1016/0016-7037(82)90153-3)

Nelson, D. M., Tréguer, P., Brzezinski, M. A., Leynaert, A., & Quéguiner, B. (1995). Production and dissolution of biogenic silica in the ocean: Revised global estimates, comparison with regional data and relationship with biogenic sedimentation. *Global Biogeochemical Cycles*, 9, 359–372.
<https://doi.org/10.1029/95GB01070>

Neven, C. J., Giraldo, C., Girardin, R., Lefebvre, A., Lefebvre, S., Loots, C., Meunier, C. L., & Marchal, P. (2024). Winter distribution of zooplankton and ichthyoplankton assemblages in the North Sea and the English Channel. *PLOS ONE*, 19(10), e0308803. <https://doi.org/10.1371/journal.pone.0308803>

Ólafsson, J., Ólafsdóttir, S. R., Benoit-Cattin, A., Danielsen, M., Arnarson, T. S., & Takahashi, T. (2009). Rate of Iceland Sea acidification from time series measurements. *Biogeosciences*, 6(11), 2661–2668.
<https://doi.org/10.5194/bg-6-2661-2009>

- Ovaskainen, O., Weigel, B., Potyutko, O., & Buyvolov, Y. (2019). Long-term shifts in water quality show scale-dependent bioindicator responses across Russia—Insights from 40 year-long bioindicator monitoring program. *Ecological Indicators*, 98, 476–482. <https://doi.org/10.1016/j.ecolind.2018.11.027>
- R Core Team. (2022). *R: A language and environment for statistical computing*. R Foundation for Statistical Computing. <https://www.R-project.org/>
- Redfield, A. C., Ketchum, B. H., & Richards, F. A. (1963). The influence of organisms on composition of seawater. In M. N. Hill (Ed.), *The Sea* (Vol. 2, pp. 26–77). New York: Interscience.
- Reid, P. C., Edwards, M., Beaugrand, G., Skogen, M., & Stevens, D. (2003). Periodic changes in the zooplankton of the North Sea during the twentieth century linked to oceanic inflow. *Fisheries Oceanography*, 12, 260–269. <https://doi.org/10.1046/j.1365-2419.2003.00252.x>
- Reimer, J. J., Cai, W.-J., Xue, L., Vargas, R., Noakes, S., Hu, X., Signorini, S. R., Mathis, J. T., Feely, R. A., Sutton, A. J., Sabine, C., Musielewicz, S., Chen, B., & Wanninkhof, R. (2017). Time series pCO₂ at a coastal mooring: Internal consistency, seasonal cycles, and interannual variability. *Continental Shelf Research*, 145, 95–108. <https://doi.org/10.5194/essd-11-421-2019>
- Richardson, A. J., & Schoeman, D. S. (2004). Climate impact on plankton ecosystems in the Northeast Atlantic. *Science*, 305(5690), 1609–1612. <https://doi.org/10.1126/science.1100958>
- Riebesell, U., Schulz, K. G., Bellerby, R. G. J., Botros, M., Fritsche, P., Meyerhöfer, M., Neil, C., Nondal, G., Wohlers, J., & Zöllner, E. (2007). Enhanced biological carbon consumption in a high CO₂ ocean. *Nature*, 450(7169), 545–548. <https://doi.org/10.1038/nature06267>
- Romero, E., Garnier, J., Billen, G., Ramarson, A., Riou, P., & Le Gendre, R. (2019). Modeling the biogeochemical functioning of the Seine estuary and its coastal zone: Export, retention, and transformations. *Limnology and Oceanography*, 64(3), 895–912. <https://doi.org/10.1002/lno.11082>
- Romero, E., Le Gendre, R., Garnier, J., Billen, G., Fisson, C., Silvestre, M., & Riou, P. (2016). Long-term water quality in the lower Seine: Lessons learned over 4 decades of monitoring. *Environmental Science & Policy*, 141–154. <http://dx.doi.org/10.1016/j.envsci.2016.01.016>
- Sala, O. E., Chapin, F. S., Armesto, J. J., Berlow, E., Bloomfield, J., Dirzo, R., Huber-Sanwald, E., Huenneke, L. F., Jackson, R. B., Kinzig, A., Leemans, R., Lodge, D. M., Mooney, H. A., Oesterheld, M., Poff, N. L. R., Sykes, M. T., Walker, B. H., Walker, M., & Wall, D. H. (2000). Global biodiversity scenarios for the year 2100. *Science*, 287, 1770–1774. <https://doi.org/10.1126/science.287.5459.1770>
- Santana-Casiano, J. M., González-Dávila, M., Rueda, M. J., Llinás, O., & González-Dávila, E. F. (2007). The interannual variability of oceanic CO₂ parameters in the northeast Atlantic subtropical gyre at the ESTOC site. *Global Biogeochemical Cycles*, 21(1). <https://doi.org/10.1029/2006GB002788>
- Sarmiento, J. L., & Gruber, N. (2006). *Ocean biogeochemical dynamics*. Princeton University Press.
- Schulz, K. G., Riebesell, U., Bellerby, R. G. J., Biswas, H., Meyerhöfer, M., Müller, M. N., Egge, J. K., Nejstgaard, J. C., Neil, C., Wohlers, J., & Zöllner, E. (2008). Build-up and decline of organic matter during PeECE III. *Biogeosciences*, 5(3), 707–718. <https://doi.org/10.5194/bg-5-707-2008>

- 680 **Selman, M., Greenhalgh, S., Diaz, R., & Sugg, Z.** (2008). *Eutrophication and hypoxia in coastal areas: A global assessment of the state of knowledge*. World Resources Institute.
- Shen, Z. L.** (2001). Historical changes in nutrient structure and its influences on phytoplankton composition in Jiaozhou Bay. *Estuarine, Coastal and Shelf Science*, 52(2), 211–224. <https://doi.org/10.1006/ecss.2000.0736>
- 685 **Simon, A., Poppeschi, C., Plecha, S., Charria, G., & Russo, A.** (2023). Coastal and regional marine heatwaves and cold spells in the northeastern Atlantic. *Ocean Science*, 19(5), 1339–1355. <https://doi.org/10.5194/os-19-1339-2023>
- SMEL - Synergie Mer & Littoral.** (2024). *Hydrobiological data from 5 stations of the HYDRONOR Observatory (2000–2024)* [Dataset]. Zenodo. <https://doi.org/10.5281/zenodo.15058835>
- 690 **Smith, V. H.** (2006). Responses of estuarine and coastal marine phytoplankton to nitrogen and phosphorus enrichment. *Limnology and Oceanography*, 51(1–2), 377–384. https://doi.org/10.4319/lo.2006.51.1_part_2.0377
- Sonier, R., Filgueira, R., Guyondet, T., Tremblay, R., Olivier, F., Meziane, T., Starr, M., LeBlanc, A. R., & Comeau, L. A.** (2016). Picophytoplankton contribution to *Mytilus edulis* growth in an intensive culture environment. *Marine Biology*, 163, 1–15.
- 695 **Strickland, J., & Parsons, T.** (1972). *A practical handbook of seawater analysis* (2nd ed., Vol. 167). Fisheries Research Board of Canada.
- Tréguer, P. J., & De La Rocha, C. L.** (2013). The world ocean silica cycle. *Annual Review of Marine Science*, 5(1), 477–501. <https://doi.org/10.1146/annurev-marine-121211-172346>
- 700 **Vermaat, J. E., McQuatters-Gollop, A., Eleveld, M. A., & Gilbert, A.** (2008). Past, present and future nutrient loads of the North Sea: Causes and consequences. *Estuarine, Coastal and Shelf Science*, 80(1), 53–59.
- Watanabe, K., Kasai, A., Fukuzaki, K., Ueno, M., & Yamashita, Y.** (2017). Estuarine circulation-driven entrainment of oceanic nutrients fuels coastal phytoplankton in an open coastal system in Japan. *Estuarine, Coastal and Shelf Science*, 184, 126–137. <https://doi.org/10.1016/j.ecss.2016.10.031>
- 705 **Yan, X., Garnier, J., Billen, G., Wang, S., & Thieu, V.** (2022). Unravelling nutrient fate and CO₂ concentrations in the reservoirs of the Seine Basin using a modelling approach. *Water Research*, 225, 119135. <https://doi.org/10.1016/j.watres.2022.119135>
- Yan, X., Thieu, V., & Garnier, J.** (2021). Long-term assessment of nutrient budgets for the four reservoirs of the Seine Basin (France). *Science of the Total Environment*, 778, 1. <https://doi.org/10.1016/j.scitotenv.2021.146412>
- 710